Hole-mediated ferromagnetism in tetrahedrally coordinated semiconductors

T. Dietl*
Research Institute of Electrical Communication, Tohoku University, Katahira 2-1-1, Sendai 980-8577, Japan and Institute of Physics and College of Science, Polish Academy of Sciences, aleja Lotników 32/46, PL-00-668 Warszawa, Poland

H. Ohno and F. Matsukura
Laboratory for Electronic Intelligent Systems, Research Institute of Electrical Communication, Tohoku University, Katahira 2-1-1, Sendai 980-8577, Japan

(Received 11 July 2000; published 19 April 2001)

A mean-field model of ferromagnetism mediated by delocalized or weakly localized holes in zinc-blende and wurzite diluted magnetic semiconductors is presented. The model takes into account strong spin-orbit and $k \cdot p$ couplings in the valence band as well as the influence of strain upon the hole density of states. Possible effects of disorder and carrier-carrier interactions, particularly near the metal-to-insulator transition, are discussed. A quantitative comparison between experimental and theoretical results for (Ga,Mn)As demonstrates that the theory describes the values of the Curie temperatures observed in the studied systems as well as explaining the directions of the easy axes and the magnitudes of the corresponding anisotropy fields as a function of biaxial strain. Furthermore, the model reproduces the unusual sign, magnitude, and temperature dependence of the magnetic circular dichroism in the spectral region of the fundamental absorption edge. Chemical trends and various suggestions concerning design of ferromagnetic semiconductor systems are described.

DOI: 10.1103/PhysRevB.63.195205 PACS number(s): 75.50.Pp, 72.80.Ey, 75.30.Hx, 75.50.Dd

I. INTRODUCTION

The discovery of ferromagnetism in zinc-blende[1,2] III-V and[3,4] II-VI Mn-based compounds allows one to explore the physics of previously unavailable combinations of quantum structure and magnetism in semiconductors. For instance, it was shown to be possible to change the magnetic phase using light in[5] (In,Mn)As/(Al,Ga)Sb and[3] (Cd,Mn)Te/(Cd,Zn,Mg)Te heterostructures. Injection of spin-polarized carriers from (Ga,Mn)As to an (In,Ga)As quantum well in the absence of an external magnetic field was also demonstrated.[6] It is thus important to understand the ferromagnetism in these semiconductors, and to ask whether the Curie temperature T_C can be raised to above 300 K from the present 110 K observed for $Ga_{0.947}Mn_{0.053}As$.[2,7]

In this paper, we develop the theory of hole-mediated ferromagnetism in tetrahedrally coordinated semiconductors along the lines of our recently proposed model.[8] Since we aim at a quantitative description of experimental findings, the proposed theoretical approach[8] makes use of empirical facts and parameters wherever possible. We begin the present paper by discussing electronic states in *p*-type magnetic semiconductors. We classify the studied systems as charge-transfer insulators, so that our theory is not applicable to materials in which d electrons participate in charge transport. We note that Mn ions act as both a source of localized spins and effective mass acceptors. We adapt, therefore, the physics of the metal-insulator transition in doped semiconductors for the case studied, and assume that over the relevant range of impurity concentrations the ferromagnetic exchange is mediated by delocalized or weakly localized holes. Since the resulting spin-spin coupling is long range, we use a mean-field approximation to determine various thermodynamic, magnetoelastic, and optical properties of the system. Particular case is used to take carefully into account the complex structure of the valence band. We then present the results of comprehensive numerical studies which provide a qualitative, and in many cases quantitative, interpretation of experimental findings accumulated over recent years for (Ga,Mn)As. This good agreement between experimental and theoretical data encourages us to show expected chemical trends in the final part of the paper, and to give various suggestions concerning the design of ferromagnetic semiconductor systems.

In general terms, our results point to the importance of the $k \cdot p$ and spin-orbit interactions in the physics of hole-mediated ferromagnetism in semiconductors. These interactions control the magnitude of the Curie temperature, the saturation value of the magnetization, and the character of magnetic anisotropies. A comparison of theoretical and experimental findings not only emphasizes similarities and differences between III-V magnetic semiconductors and other ferromagnetic systems, but also demonstrates different aspects of half-metallic ferromagnets. Recent comprehensive reviews present many aspects of III-V,[9] II-VI,[10] as well as IV-VI magnetic semiconductors,[11] which will not be discussed here.

II. ELECTRONIC STATES IN *p*-TYPE MAGNETIC SEMICONDUCTORS

A. Mn ion in tetrahedrally coordinated semiconductors

We consider zinc-blende or wurzite semiconductor compounds, in which the cations are partly substituted by magnetic ions, such as Mn. The magnetic ions are assumed to be randomly distributed over the cation sites, as found by extended x-ray absorption fine structure studies of $Ga_{1-x}Mn_xAs$ (Ref. 12) and $Cd_{1-x}Mn_xTe$.[13] The Mn pro-

vides the localized spin $S=\frac{5}{2}$ and, in the case of III-V semiconductors, acts as an acceptor. These Mn acceptors compensate the deep antisite donors commonly present in GaAs grown by low-temperature molecular beam epitaxy, and produce a *p*-type conduction with metallic resistance for the Mn concentration x in the range $0.04 \leqslant x \leqslant 0.06$.[7,14–16] Accurate analysis of the transport data, complicated by the large magnitude of the anomalous Hall effect, confirms the presence of a strong compensation,[17] presumably by As antisite donors, as mentioned above. However, at this stage we cannot exclude the existence of self-compensation mechanisms, such as the formation of Mn *AX*-like centers or donor defects once the Fermi level reaches an appropriately deep position in the valence band.[18]

According to optical studies, Mn in GaAs forms an acceptor center characterized by a moderate binding energy[19] $E_a = 110$ meV, and a small magnitude of the energy difference between the states corresponding to the spin of the bound hole parallel and antiparallel to the Mn spin,[19,20] $\Delta\epsilon = 8 \pm 3$ meV. This small value demonstrates that the hole introduced by the divalent Mn in GaAs does not reside on the d shell or form a Zhang-Rice-like singlet,[21,22] but occupies an effective-mass Bohr orbit.[8,23] Thus, due to the large intrasite correlation energy U, (Ga,Mn)As can be classified as a charge-transfer insulator, a conclusion consistent with photoemission spectroscopy.[24,25] At the same time, the *p-d* hybridization results in a spin-dependent coupling between the holes and the Mn ions, $H_{pd} = -\beta N_0 \mathbf{s}\cdot\mathbf{S}$. Here β is the *p-d* exchange integral and N_0 is concentration of the cation sites. Analysis of photoemission data[24,25] and the magnitude[23] of $\Delta\epsilon$ leads to the exchange energy $\beta N_0 \approx -1$ eV. Similar values of βN_0 are observed in II-VI diluted magnetic semiconductors with comparable lattice constants.[26] This confirms Harrison's suggestion that the hybridization matrix elements depend primarily on the interatomic distance.[27] According to the model in question, the magnetic electrons remain localized at the magnetic ion, so that they do not contribute to charge transport. This precludes Zener's double exchange[28] as the mechanism leading to ferromagnetic correlation between the distant Mn spins. At the same time, for some combinations of transition metals and hosts, the ''chemical'' and exchange attractive potential introduced by the magnetic ion can be strong enough to bind the hole in a local orbit.[21,22] In an intermediate regime, the probability of finding the hole around the magnetic ion is enhanced, which results in the apparent increase of $|\beta N_0|$ with decreasing x.[22]

B. Two-fluid model of electronic states near the metal-insulator transition

Ionized impurity and magnetic scattering lead to localization of the effective-mass holes introduced by Mn in III-V compounds or by acceptors in the case of II-VI materials. It is therefore important to discuss the effect of Anderson-Mott localization on the onset of ferromagnetism. The two-fluid model[29] constitutes the established description of electronic states in the vicinity of the Anderson-Mott metal-insulator transition (MIT) in doped semiconductors. According to that model, the conversion of itinerant electrons into singly occupied impurity states with increasing disorder occurs gradually, and has already begun on the metal side of the MIT. This leads to a disorder-driven static phase separation into two types of region, one populated by electrons in extended states, and another that is totally depleted of carriers or contains singly occupied impuritylike states. The latter region controls the magnetic response of doped nonmagnetic semiconductors[29] and gives rise to the presence of bound magnetic polarons (BMP's) on both sides of the MIT in magnetic semiconductors.[26,30,31] Actually, the formation of BMP's shifts the MIT toward higher carrier concentrations.[26,30,31] On crossing the MIT, the extended states become localized. However, according to the scaling theory of the MIT, their localization radius ξ decreases rather gradually from infinity at the MIT toward the Bohr radius deep in the insulator phase, so that on a length scale smaller than ξ the wave function retains an extended character. Such weakly localized states are thought to determine the static longitudinal and Hall conductivities of doped semiconductors. The central suggestion of the recent model[8] is that the holes in extended or weakly localized states mediate the long-range interactions between the localized spins on both sides of the MIT in the III-V and II-VI magnetic semiconductors.

As will be discussed below, the Curie temperature T_C is proportional to the thermodynamic spin density of states ρ_s, which, in turn, is proportional to the spin susceptibility of the carrier liquid, χ_s. Like other thermodynamic quantities, ρ_s does not exhibit any critical behavior at the MIT. However, ρ_s exhibits large space fluctuations at criticality, which will result in local fluctuations of magnetic properties. The quantitative renormalization of ρ_s by disorder will depend on its microscopic nature, for instance, on the degree of compensation. The enhancement of ρ_s by the carrier-carrier interactions can be described by the Fermi-liquid parameter A_F, $\rho_s \rightarrow A_F \rho_s$.[32] The value of $A_F = 1.2$, as evaluated[33] by the local-spin-density approximation for the relevant hole concentrations, has been adopted for our computations. We note that disorder-modified carrier-carrier interactions in the triplet particle-hole channel tend to enhance A_F, which may even drive the system toward a Stoner-like instability.[34] In magnetic systems, however, spin-flip scattering by fluctuations of magnetization makes this enhancement mechanism rather inefficient.

The two-fluid model is consistent with recent electron paramagnetic resonance (EPR) results,[35] which show the coexistence of the neutral Mn acceptors and ionized Mn d^5 states in some range of Mn concentration. Furthermore, the observed[36,37] sign of the magnetic circular dichroism in (Ga,Mn)As suggests the presence of Fermi-liquid-like states on both sides of the MIT, as we shall discuss in Sec. IV D.

C. Valence band structure and exchange splitting of the hole subbands

Since the valence band originates merely from the anion p and cation d wave functions, the exchange interaction mediated by holes is expected to be strongly affected by anisotropy of hole dynamics and the coupling between the spin and

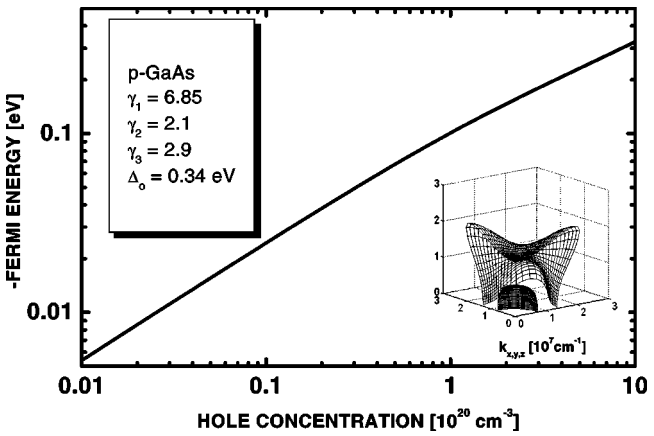

FIG. 1. Fermi energy as a function of the hole concentration p computed from the 6×6 Luttinger model for $k\cdot p$ parameters displayed in the figure. Inset shows cross section of the Fermi sphere for $p=3.5\times10^{20}$ cm^{-3}.

orbital degrees of freedom. To take those effects into account, the hole dispersion and wave functions are computed by diagonalizing the 6×6 Kohn-Luttinger $k\cdot p$ matrix.[38] In this model, four Γ_8 and two Γ_7 bands are taken explicitly into account, whereas other bands are included by second-order perturbation theory. The model is developed for zinc-blende and wurzite semiconductors. It allows for warping, quantizing magnetic fields, and biaxial strain, but no terms associated with the lack of symmetry inversion are taken into account. The effect of the spin-dependent interaction between the holes and the Mn spins is described in terms of the virtual-crystal and molecular-field approximations,[39] so that

$$H_{pd}=\beta\mathbf{s}\cdot\mathbf{M}(\mathbf{r})/g\mu_B, \tag{1}$$

where $\mathbf{M}(\mathbf{r})$ is the magnetization of the localized spins that carry magnetic moment $-Sg\mu_B$, where $S=\frac{5}{2}$ and $g=2.0$.

The explicit form of the $k\cdot p$ 6×6 matrices, together with the matrix $H_{\rm pd}$ derived by us in the Luttinger-Kohn representation for arbitrary directions of magnetization $\mathbf{M}$, are displayed in Appendix A. We note that for the case under consideration, involving large exchange interaction and high kinetic energy, particularly important are off-diagonal terms describing the p-d coupling between the Γ_8 and Γ_7 bands. A numerical procedure that serves to determine the concentration, free energy, wave functions, and optical characteristics of the holes is outlined in Appendix B. The adopted values of the Luttinger parameters γ_i and the spin-orbit splittings Δ_0 are summarized in Appendix C for various III-V and II-VI parent compounds. According to photoemission studies[24] $\beta N_0=-1.2\pm0.2$ eV for (Ga,Mn)As. The value $\beta N_0=-1.2$ eV is taken for the computations, although future work may reveal some dependence of β in Eq. (1) on Mn and/or hole concentrations because of the energetic proximity of the Fermi and relevant Mn d levels. Such a dependence could result also from corrections to the virtual-crystal and molecular-field approximations if the short-range part of the Mn potential is attractive for the valence band hole.[22]

Figure 1 presents the dependence of the low-temperature Fermi energy ε_F on the hole concentration p computed for the band parameters corresponding to GaAs. No effects of p-d exchange, disorder, or Coulomb interactions between the holes are taken into account. The corresponding density-of-states (DOS) effective mass increases from $0.67m_0$ in the limit of small hole concentrations to the value of $1.35m_0$ for $p=5\times10^{20}$ cm^{-3}. This increase is caused by the $k\cdot p$ interaction between the Γ_8 and Γ_7 bands, which—because of the relatively small magnitude of Δ_0 in GaAs—is important for the relevant hole densities. The inset to Fig. 1 shows the cross section of the Fermi surface for $p=3.5\times10^{20}$ cm^{-3}, which corresponds to $\varepsilon_F=-195$ meV with respect to the energy of the Γ_8 point. Two valleys, the heavy- and light-hole subbands, are visible.

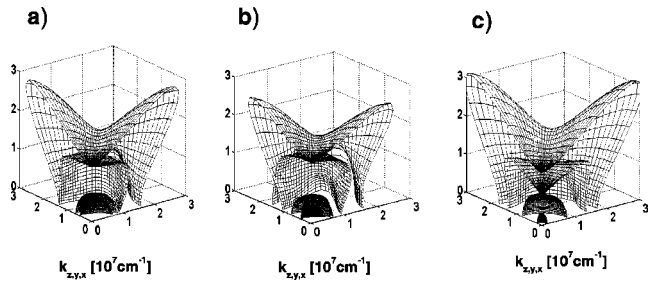

FIG. 2. Cross sections of the Fermi spheres for saturation value of magnetization M in $Ga_{0.95}Mn_{0.05}As$ with hole concentration $p=3.5\times10^{20}$ cm^{-3}. Results for various orientations of magnetization $\mathbf{M}$ and biaxial strains ϵ_{xx} are shown: (a) $M\|$ [100]; $\epsilon_{xx}=0$; (b) $M\|$ [100]; $\epsilon_{xx}=-2\%$; (c)$M\|$ [001]; $\epsilon_{xx}=+2\%$. A strong dependence of the splitting on the relative orientation of the wave vector and magnetization is visible.

A strong and complex influence of the p-d interaction and strain upon the valence band is shown in Fig. 2. The cross sections of the Fermi spheres are depicted for $p=3.5\times10^{20}$ cm^{-3}, which now corresponds to $\varepsilon_F\approx-165$ meV, and for the parameter of the exchange splitting,

$$B_G=A_F\beta M/6g\mu_B, \tag{2}$$

taken as $B_G=-30$ meV. If $\beta N_0=-1.2$ eV and $A_F=1.2$, this magnitude of B_G occurs for the saturation value of magnetization M at $x=0.05$. We note at this point that some of the effects, e.g., the direction of the spin-polarization vector, depend on the sign of β and thus B_G, whereas others, like the Curie temperature, are proportional to β^2. In the absence of strain, $\epsilon=0$, the fourfold degeneracy at the Γ point is lifted by the p-d exchange, and the corresponding energies at $k=0$ are $\pm3B_G$ and $\pm B_G$ for $\Delta_0\gg|B_G|$. However, the splitting at nonzero wave vectors depends on the relative orientation of $\mathbf{M}$ and $\mathbf{k}$.[39] In particular, since the spin of the heavy hole is polarized along $\mathbf{k}$ for $\epsilon=0$, the exchange splitting is seen to vanish for $\mathbf{k}\perp\mathbf{M}$. This mixing of orbital and spin degrees of freedom, together with highly nonparabolic, anisotropic, and mutually crossing dispersion relations, constitute important aspects of the hole-mediated ferromagnetism in terahedrally coordinated semiconductors.

III. HOLE-INDUCED FERROMAGNETISM IN SEMICONDUCTORS

A. Short-range antiferromagnetic superexchange and ferromagnetic double exchange

In addition to the interaction between the carrier and localized spin subsystems, the p-d hybridization leads also to superexchange, a short-range antiferromagnetic coupling between the Mn spins. The superexchange is mediated by spin polarization of occupied electron bands, in contrast to the Zener ferromagnetic exchange, which is mediated by spin polarization of the carrier liquid. The antiferromagnetic exchange dominates in undoped II-VI semiconductors,[26] and also in compensated $Ga_{1-x}Mn_xAs:Sn$.[40] Based on qualitative considerations presented below, the presence of this interaction is taken into account in the case of II-VI materials but neglected in the case of noncompensated (Ga,Mn)As structures.

It is convenient to parametrize the dependence of magnetization on the magnetic field in the absence of the carriers, $M_0(H)$, by the Brillouin function B_S according to

$$M_0(H) = g\mu_B S N_0 x_{\rm eff} B_S[g\mu_B H/k_B(T+T_{AF})], \qquad (3)$$

where two empirical parameters, the effective spin concentration $x_{\rm eff}N_0 < xN_0$ and temperature $T_{\rm eff} > T$, take the presence of the superexchange antiferromagnetic interactions into account.[26,41] The dependencies $x_{\rm eff}(x)$ and $T_{\rm AF}(x) \equiv T_{\rm eff}(x) - T$ are known[42,41] for II-VI compounds.

In order to elucidate the effect of doping on $x_{\rm eff}$ and $T_{\rm AF}$ we refer to the two-fluid model described in Sec. II B. In terms of that model the delocalized or weakly localized holes account for the ferromagnetism. In fact, the participation of the same set of holes in both charge transport and ferromagnetic interactions is shown, in (Ga,Mn)As (Ref. 14) and in (Zn,Mn)Te,[43] by the agreement between the temperature and field dependencies of the magnetization deduced from the anomalous Hall effect, M_H, and from direct magnetization measurements, M_D, particularly in the vicinity of T_C. However, below T_C and in magnetic fields greater than the coercive force, while M_H saturates (as in standard ferromagnets), M_D continues to increase with increasing magnetic field.[14,37] Since M_H is proportional to the spin polarization of the carriers, its saturation may reflect a saturation of hole polarization, which—for appropriately low values of the Fermi energy—can occur even if the Mn spins are not totally spin polarized (half-metallic case). It appears, however, that Mn spins in the regions depleted of carriers (which, therefore, do not participate in the long-range magnetic order) also contribute to the slowly increasing component of $M_D(H)$.

According to the two-fluid model, some of the carriers are trapped on strongly localized impurity states, and thus form bound magnetic polarons. If there is an exchange coupling between the two fluids, the BMP's participate in the formation of ferromagnetic order. Furthermore, the coupling between the BMP's appears to be ferromagnetic, at least in some range of relevant parameters.[44,45] To gain Coulomb energy, the BMP's are preferentially formed around close pairs of ionized acceptors. In the case of III-V materials this leads, via Zener's double exchange,[46] to a local ferromagnetic alignment of neighbor Mn d^5 negative ions,[47] so that $x \approx x_{\rm eff}$ and $T_{\rm AF} \approx 0$. By contrast, in II-VI compounds, for which acceptor cores do not carry any spin and the degree of compensation is low, BMP's are not preferentially formed around Mn pairs, so that the close pairs remained antiferromagnetically aligned, even in p-type samples. The presence of competition between the ferromagnetic and antiferromagnetic interactions in II-VI compounds, and its absence in III-V materials, constitutes an important difference between these two families of magnetic semiconductors.

B. Zener model of ferromagnetic interactions mediated by free carriers

As mentioned above, we assume that weakly localized or delocalized holes mediate long-range ferromagnetic interaction between the spins. Zener[46] first proposed a model of ferromagnetism driven by the exchange coupling of the carriers and the localized spins. According to that model, spin polarization of the localized spins leads to spin splitting of the bands, which results in the lowering of the carrier energy. At sufficiently low temperature, this lowering overcompensates the increase of the free energy caused by the decrease of entropy, that is associated with the polarization of localized spins. However, the Zener model was later abandoned, as neither the itinerant character of the magnetic electrons nor the quantum (Friedel) oscillations of the electron spin polarization around the localized spins were taken into account, and both of these are now established to be critical ingredients of the theory of magnetic metals. In particular, the resulting competition between ferromagnetic and antiferromagnetic interactions in metals leads rather to a spin-glass than to a ferromagnetic ground state. In the case of semiconductors, however, the mean distance between the carriers is usually much greater than that between the spins. Under such conditions, the exchange interaction mediated by the carriers is ferromagnetic for most of the spin pairs, which reduces the tendency toward spin-glass freezing. In fact, for a random distribution of the localized spins, the mean-field value of the Curie temperature T_C deduced from the Zener model is equal to that obtained from the Ruderman, Kittel, Kasuya, and Yosida (RKKY) approach,[32,48–50] in which the presence of the Friedel oscillations is explicitly taken into account.

C. Mean-field model of Curie temperature and thermodynamic properties

As reported elsewhere,[8] the Zener model describes correctly the experimental values of T_C in both (Ga,Mn)As and (Zn,Mn)Te, provided that band structure effects are taken into account. The starting point of the model is to determine how the Ginzburg-Landau free-energy functional F depends on the magnetization M of the localized spins. The hole contribution to F, $F_c[M]$, is computed by diagonalizing the 6×6 Kohn-Luttinger matrix together with the p-d exchange contribution, and by subsequent computation of the partition function Z, as described in Appendix B. This model takes the effects of the spin-orbit interaction into account, a task difficult technically within the RKKY approach, as the spin-orbit coupling leads to nonscalar terms in the spin-spin

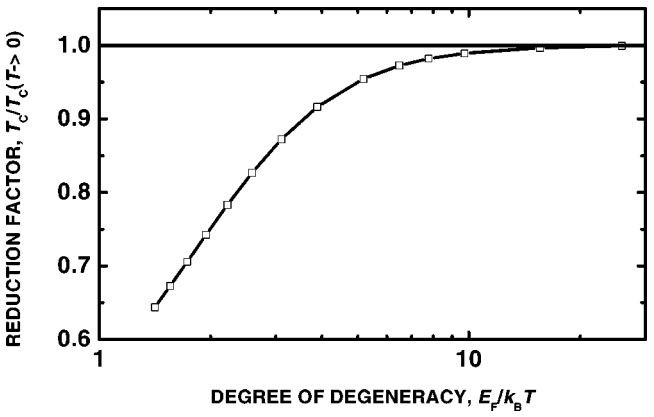

FIG. 3. The computed ratio of the actual Curie temperature T_C to that obtained assuming that the hole liquid is strongly degenerate as a function of the degeneracy factor.

Hamiltonian. Moreover, the indirect exchange associated with the virtual spin excitations between the valence subbands, the Bloembergen-Rowland mechanism[26] is automatically included. The remaining part of the free-energy functional, that of the localized spins, is given by

$$F_S[M]=\int_0^M dM_0 H(M_0), \tag{4}$$

where $H(M_0)$ is given in Eq. (3). By minimizing $F[M]=F_c[M]+F_S[M]$ with respect to M at given T, H, and hole concentration p, one obtains $M(T,H)$ as a solution of the mean-field equation,

$$M=\mu_g\mu_B S N_0 x_{\rm eff} \mathrm{B}_S\left[\frac{g\mu_B(-\partial F_c[M]/\partial M+H)}{k_B(T+T_{\rm AF})}\right]. \tag{5}$$

Near the Curie temperature T_C, where M is small, we expect $F_c[M]-F_c[0]\sim M^2$. It is convenient to parametrize this dependence by the spin density of states ρ_s,

$$F_c[M]=F_c[0]-A_F\rho_s\beta^2M^2/2(2g\mu_B)^2. \tag{6}$$

The spin density of states ρ_s is related to the carrier magnetic susceptibility according to $\chi=A_F(g^*\mu_B)^2\rho_s/4$ and, in general, has to be determined numerically by computing $F_c[M]$. By expanding $\mathrm{B}_S(M)$ we arrive at,

$$T_C=x_{\rm eff}N_0S(S+1)\beta^2A_F\rho_s(T_C)/12k_B-T_{\rm AF}. \tag{7}$$

For a strongly degenerate carrier liquid, $|\varepsilon_F|/k_BT\gg 1$, and neglecting the spin-orbit interaction, ρ_s becomes equal to the total density of states ρ for intraband charge excitations, where $\rho=m^*_{\rm DOS}k_F/\pi^2\hbar^2$.

In order to check the quantitative significance of carrier entropy, the computed values of T_C were compared to those obtained assuming strong degeneracy of the carrier liquid. As shown in Fig. 3 such an assumption leads to error smaller than 1% if $\varepsilon_F|/k_BT>10$. Thus, in this range, the carrier energy, not the free energy, was used for the evaluation of T_C. Furthermore, we take $x_{\rm eff}=x$ and $T_{\rm AF}=0$, as discussed above.

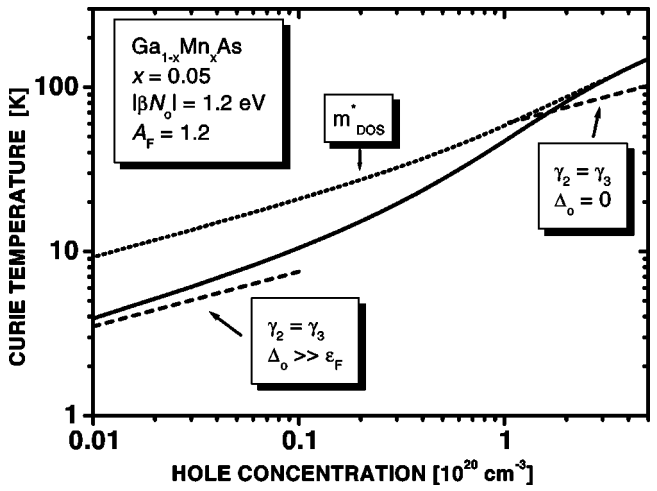

FIG. 4. Curie temperature as a function of the hole concentration for $Ga_{0.95}Mn_{0.05}As$ computed from the 6×6 Luttinger model (solid line). Straight dashed lines represent results obtained assuming a large and a small value of the spin-orbit splitting Δ_0, respectively. The dotted line is calculated neglecting the effect of the spin-orbit interaction on the hole spin susceptibility.

The values of T_C as a function of the hole concentration p for $Ga_{0.95}Mn_{0.05}As$, as computed by our model, are shown by the solid line in Fig. 4. Since the magnitude of T_C is directly proportional to $x_{\rm eff}N_0\beta^2A_F$, the theoretical results can easily be extended to other values of x, β, or A_F. In particular, $T_C=300$ K is expected for $x=0.125$ and $p=3.5\times10^{20}$ cm^{-3}.

D. Validity of the model and comparison to other approaches

Equation (7) with $\rho_s=\rho$, that is, neglecting the effects of spin-orbit interaction, has already been derived by a number of equivalent methods.[26,32,33,48] In the present work $F_c[M]$, which served to determine T_C, $M(T,H)$, the anisotropy fields, and the optical spectra, was obtained from the 6×6 $k\cdot p$ model, as described in Appendices A and B. In order to illustrate the importance of band structure effects, the evaluation of T_C has been performed employing various models. The two straight dashed lines in Fig. 4 depict the expected $T_C(p)$ if the warping is neglected ($\gamma_2=\gamma_3$) and a large and a small spin-orbit splitting $E_{\Gamma_8}-E_{\Gamma_7}\equiv\Delta_0$ is assumed, respectively. We see that the above assumptions are approximately fulfilled in the low and high concentration ranges, but the calculation within the full model is necessary in the experimentally relevant region of intermediate hole densities. In particular, the 4×4 model[43,51] ($\Delta_0\gg|\varepsilon_F|$) would be reasonably correct for (Zn,Mn)Te, where Δ_0 is about 1 eV, but not for (Ga,Mn)As, for which Δ_0 is almost three times smaller. Finally, the dotted line shows T_C evaluated by replacing ρ_s by ρ. We see that $\rho\approx\rho_s$ already for $p\approx10^{20}$ cm^{-3}, despite the fact that $|\varepsilon_F|$ is still two times smaller than Δ_0. In contrast, ρ_s is more than two times smaller than ρ in the limit of small p. This reduction of the spin susceptibility, and thus of T_C, stems from the absence of exchange splitting of the heavy-hole subband for $\mathbf{k}\perp\mathbf{M}$.

As described above, T_C can be computed by minimizing the free energy, and without referring to the explicit form of the Kohn-Luttinger amplitudes $u_{i\mathbf{k}}$. Since near T_C the relevant magnetization M is small, the carrier free energy, and thus T_C, can also be determined from linear response theory. The corresponding ρ_s assumes the standard form

$$\rho_s = \lim_{q\to 0} 8 \sum_{ij\mathbf{k}} \frac{|\langle u_{i,\mathbf{k}}|s_M|u_{j,\mathbf{k}+\mathbf{q}}\rangle|^2 f_i(\mathbf{k})[1-f_j(\mathbf{k}+\mathbf{q})]}{E_j(\mathbf{k}+\mathbf{q})-E_i(\mathbf{k})}, \tag{8}$$

where s_M is the component of the spin operator along the direction of magnetization and $f_i(\mathbf{k})$ is the Fermi-Dirac distribution function for the ith valence subband. The equivalence of ρ_s as given by Eqs. (6) and (8) can be checked for the 4×4 spherical model by using the explicit forms[52] of $E_i(k)$ and u_i. Such a comparison demonstrates that almost a 30% contribution to T_C originates from interband polarization.

As discussed elsewhere[32,48,50] it is straightforward to generalize the model for the case of carriers confined to a d-dimensional space. The tendency toward the formation of spin-density waves in low-dimensional systems[48,53] as well as possible spatial correlation in the distribution of the magnetic ions can also be taken into account within the formalism considered here.

Since within the mean-field approximation (MFA) the presence of magnetization fluctuations is neglected, our model may lead to an overestimation of the magnitude of M, and thus of T_C. To address this question we recall that the decay of the strength of the carrier-mediated exchange interaction with increasing distance between the spins r is described by the RKKY function, which in the three-dimensional situation assumes the form,[48–50]

$$J(r)\sim[\sin(2k_F r)-2k_F r\cos(2k_F r)]/(2k_F r)^4. \tag{9}$$

In the case of semiconductors the average distance between the carriers $r_c=(4\pi p/3)^{-1/3}$ is usually much greater than that between the spins $r_S=(4\pi x N_0/3)^{-1/3}$. This means that the carrier-mediated interaction is ferromagnetic and effectively long range for most of the spins as the first zero of the RKKY function occurs at $r\approx 1.17 r_c$. A theoretical study[54] of critical exponents for a d-dimensional space showed that as long as $\sigma<d/2$ in the dependence $J(r)\sim 1/r^{d+\sigma}$ the mean-field approach to the long-wavelength susceptibility $\chi(T)$ is valid, a conclusion presumably not affected by disorder in the spin distribution. At the same time, both the relevant length scale r_c, (not r_S) and the critical exponents[54] $\eta=2-\sigma$ and $\nu=1/\sigma$ point to much faster decay of $\chi(q)$ with q than that expected from the classical Ornstein-Zernike theory.[55] This indicates that the MFA should remain valid down to at least $|T-T_C|/T_C\approx r_S/r_c\ll 1$. Actually, the decay of $\chi(q)$ with q in the range $0<q<2k_F$ is corroborated by the observation of smaller critical scattering of the holes by magnetization fluctuations than that calculated for $\chi(q)=\chi(0)$.[17]

Recently, Monte Carlo studies of carrier-mediated ferromagnetism in semiconducors have been initiated.[56,57] Such an approach has the potential to test the accuracy of the MFA and to determine the actual spin configuration corresponding to the ground state. Preliminary results appear to confirm the validity of the MFA,[56,57] as well as to indicate the possibility of the existence of noncollinear magnetic structures in low-dimensional systems.[57] Another significant recent development[58] is the examination of spin-wave excitations, their spectrum and effect on magnetization. A strong reduction of T_C was predicted,[58] though it should be noted that the spin-wave approximation usually breaks down at criticality. In contrast, such an approach offers valid results at low temperatures, provided that effects of magnetic anisotropy are thoroughly taken into account. Furthermore, the existence of a ferromagnetic ground state was confirmed by *ab initio* total-energy computations for magnetic III-V compounds.[28,59,60] However, to what extent the procedures employed are able to capture correlation effects on the open d shells accurately seems to be still unclear.

Finally, we would like to stress once more that, if the concentrations of carriers and spins become comparable, $r_c \leqslant r_S$, randomness associated with the competition of ferromagnetic and antiferromagnetic interactions can drive the system toward a spin-glass phase.[61] In the case of II-VI compounds, the antiferromagnetic component is additionally enlarged by the superexchange interaction.[43] Furthermore, scattering by ionized impurities, and the associated nonuniform distribution of carriers in semiconductors near the MIT, may enhance disorder effects even further. We note also that in the extreme case $r_c \ll r_S$ the Kondo effect, that is, dynamic screening of the localized spins by the sea of carriers, may preclude both ferromagnetic and spin-glass magnetic ordering.

IV. COMPARISON OF THEORETICAL AND EXPERIMENTAL RESULTS FOR (Ga,Mn)As

A. Curie temperature and spontaneous magnetization

The most interesting property of $Ga_{1-x}Mn_xAs$ epilayers is the large magnitude of T_C, up to 110 K for the Mn concentration $x=5.3\%$.[2,7] Because of this high T_C, the spin-dependent anomalous contribution to the Hall resistance R_H persists up to 300 K, making an accurate determination of the hole density difficult.[7,14–16] However, the recent measurement[62] of R_H up to 27 T and at 50 mK yielded an unambiguous value of $p=3.5\times 10^{20}$ cm^{-3} for the metallic $Ga_{0.947}Mn_{0.053}As$ sample in which $T_C = 110$ K is observed.[7] The above value of p is about three times smaller than xN_0, confirming the importance of compensation in (Ga,Mn)As. As shown in Fig. 4, the numerical results lead to $T_C=120$ K for $x=0.05$, and thus $T_C=128$ K for $x=0.053$ and $p=3.5\times 10^{20}$ cm^{-3}. We conclude that the proposed model, with the presently known set of material parameters, describes the high values of T_C found in (Ga,Mn)As. Furthermore, the scaling theory of electronic states near the MIT, discussed in Sec. II B, makes it possible to explain the presence of the ferromagnetism on both sides of the MIT, and a noncritical evolution of T_C across the critical point.[7] A comparison between theoretical and experimental data in a wider range of Mn and hole concentrations requires reliable information on

the hole density in particular samples, which is not presently available in the case of (Ga,Mn)As.

In the case of (Zn,Mn)Te:N, the hole concentration can readily be determined by Hall effect measurements at 300 K.[4,43] The absence of the anomalous Hall effect at 300 K stems from the much lower values of T_C, $0.75 \leqslant T_C \leqslant 2.4$ K for $5\% \geqslant x \geqslant 2\%$ and $10^{19} \leqslant p \leqslant 10^{20}$ cm^{-3}. The model in question satisfactorily explains $T_C(x,p)$.[43] Three effects conspire to make T_C much greater in p-(Ga,Mn)As than in p-(Zn,Mn)Te at given p and x. First, as already mentioned, the small value of the splitting Δ_0 makes the reduction of T_C by spin-orbit coupling of minor importance in the case of (Ga,Mn)As. Second, because of the smaller lattice parameter, the product βN_0 is greater in (Ga,Mn)As. Finally, ferromagnetic double exchange between close-lying pairs of Mn ions is stronger than antiferromagnetic superexchange in compensated (Ga,Mn)As. In contrast, antiferromagnetic superexchange remains significant in p-(Zn,Mn)Te, as the Mn atoms are electrically inactive in II-VI compounds.

Important characteristics of ferromagnets are the magnitude and temperature dependence of the spontaneous magnetization M below T_C. Experimental studies of metallic samples indicate that on lowering temperature M increases as the Brillouin function reaching the saturation value M_s for $T \to 0$.[7] This behavior indicates that the molecular field H^* acting on the Mn spins is proportional to their magnetization M. Figure 5 presents values of M/M_s as a function of T/T_C calculated with no adjustable parameter for (Ga,Mn)As containing various hole and Mn concentrations. We see that indeed the computed Mn spin magnetization $M(T)/M_s$ follows, to a good approximation, the Brillouin function, except for materials with rather small values of p or large values of x. The latter cases correspond to the half-metallic situation, for which only the ground-state hole subband is populated even at $M < M_s$, so that the molecular field produced by the carriers H^* attains its maximum value and, therefore, ceases to be proportional to M. Nevertheless, the saturation value M_s can be reached provided that the temperature is sufficiently low, $k_B T_{\rm eff} \ll Sg\mu_B H^*$. Such half-metallic behavior is observed in the case of ferromagnetic correlation imposed by a dilute hole liquid in (Cd,Mn)Te quantum wells.[53]

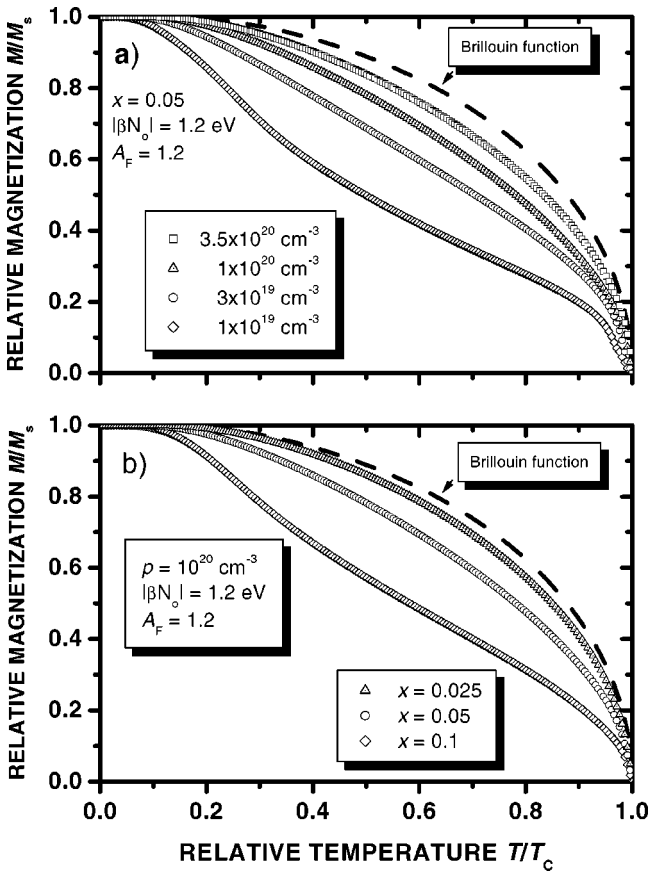

FIG. 5. The computed spontaneous magnetization M below the Curie temperature T_C for various hole concentrations p (a) and Mn content x (b) in $Ga_{0.95}Mn_{0.05}As$ (points). If the exchange splitting of the valence band is much smaller than the Fermi energy (large p, small x), the evolution of magnetization follows the Brillouin function (dashed lines).

B. Hole magnetization and spin polarization

The magnitude of the magnetization presented in the previous section was computed neglecting the possible contribution originating from hole magnetic moments. Such a contribution can be significant as the hole liquid is spin polarized for nonzero magnetization of the Mn spins. Because of the spin-orbit interaction, the hole magnetization consists of two components. One comes from the magnetic moments of the hole spins, described by the Landé factor of the free electrons and the Luttinger parameter κ. Another contribution, absent for localized carriers, originates from diamagnetic currents, whose magnetic moments can be oriented along the spin polarization by the spin-orbit interaction. Evaluation of the latter requires the inclusion of the Landau quantization in the $k \cdot p$ Hamiltonian. The carrier magnetization M_c is then given by

$$M_c = -\lim_{T,H \to 0} \partial G_c(H)/\partial H, \tag{10}$$

where the Gibbs thermodynamic potential is calculated for a given value of the Mn spin magnetization M and the Fermi energy $\varepsilon_F(M)$ as a function of the magnetic field acting on the carriers, H. In general, the eigenvalue problem for the holes in the magnetic field cannot be transformed into an algebraic equation. Such a transformation is possible, however, if the warping is neglected. We have therefore calculated the hole magnetization M_c disregarding the anisotropy, that is, assuming $\gamma_1 = 6.85$, $\gamma_2 = \gamma_3 = 2.58$, and $\kappa = 1.2$. The explicit form of the relevant Luttinger matrices is displayed in Appendix A. The partition function Z was computed by summing over the Landau index n, the wave vector k_z, and the six hole subbands.

The results of the computations are shown in Fig. 6, where M_c is plotted as a function of p for $B_G = A_F \beta M/6g\mu_B = -30$ meV. In this paper, for the sake of comparison with experimental results, we depict the magnetization in SI units according to $\mu_0 M$ (T) $= 4\pi 10^{-4} M$ (emu). The diamagnetic (orbital) contribution to M_c is seen to be negative and dominant. The spin term is positive,

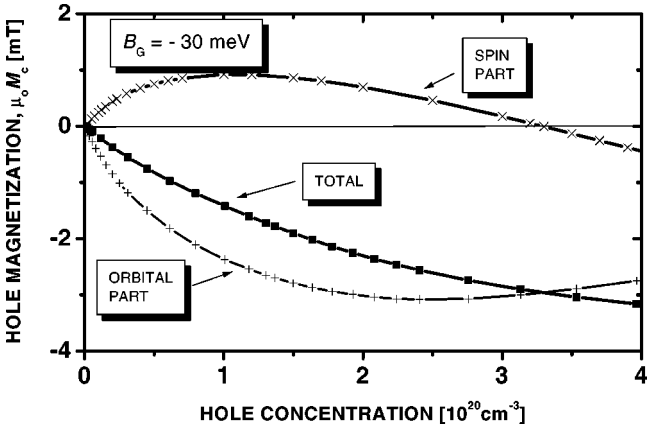

FIG. 6. Magnetization M_c of the hole liquid (squares) in $Ga_{1-x}Mn_xAs$ computed as a function of the hole concentration for the spin splitting parameter $B_G=-30$ meV (which corresponds to the saturation value of Mn spin magnetization M for $x=0.05$). Crosses show spin and orbital contributions to M_c.

which for the antiferromagnetic sign of the p-d exchange integral β indicates the negative sign of the hole Landé factor g_h. The visible decrease of the spin contribution for large p corresponds to a crossover to the free-electron value $g=2.0$ occurring when $|\varepsilon_F|$ approaches Δ_0. In Fig. 7, M_c is plotted versus M for various p. It is seen that for the values of the parameters employed, M_c reaches only 5% of $\mu_0 M=65$ mT, which corresponds to the saturation value of Mn magnetization for $x=0.05$. The rather weak magnitude of M_c results from a partial compensation of the spin and orbital contributions to M_c as well as from smaller concentration and spin of the holes in comparison to those of Mn ions. We conclude that delocalized or weakly localized holes give a minor contribution to the total magnetization. Accordingly, M_c is neglected when determining the direction of the easy axes and the magnitude of the anisotropy fields.

In view of the ongoing experiments[6] on electrical spin injection from (Ga,Mn)As, the important question arises: what is the degree of hole spin polarization $\mathcal{P}$ as a function

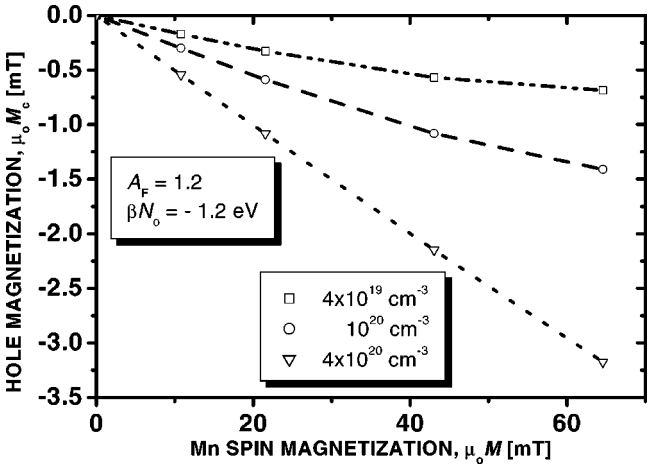

FIG. 7. Computed hole magnetization M_c as a function of Mn spin magnetization M for various hole concentrations in $Ga_{1-x}Mn_xAs$.

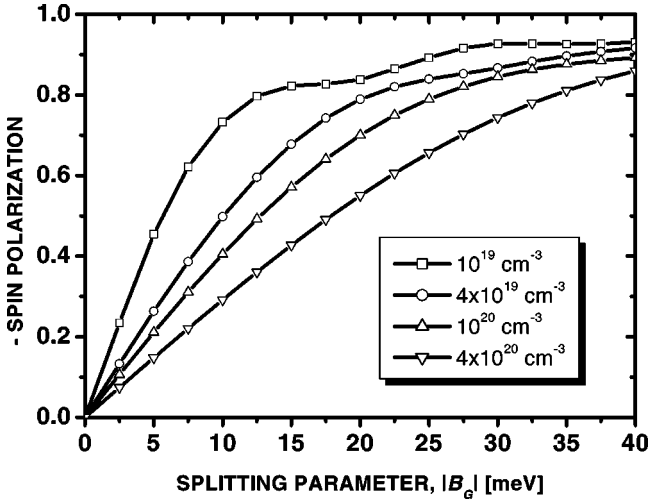

FIG. 8. Computed degree of spin polarization of the hole liquid as a function of the spin-splitting parameter for various hole concentrations in $Ga_{1-x}Mn_xAs$ ($B_G=-30$ meV corresponds to the saturation value of Mn spin magnetization for $x=0.05$). The polarization of the hole spins is oriented in the opposite direction to the polarization of the Mn spins.

of p and B_G? Furthermore, $\mathcal{P}$ appears to control the magnitude of the anomalous Hall effect. It is therefore interesting to determine the conditions under which the usual assumption about the linear relation between $\mathcal{P}$ and the magnetization of the Mn spins M is fulfilled.

The contribution of all four hole subbands to the Fermi cross section visible in Fig. 2 indicates that the exchange splitting is too small to lead to total spin polarization for $p=3.5\times10^{20}$ cm^{-3} and $x=0.05$ ($|B_G|=30$ meV). Furthermore, a destructive effect of the spin-orbit interaction on the magnitude of $\mathcal{P}$ can be expected. In order to evaluate $\mathcal{P}\equiv 2\langle s_M\rangle/p$ we note that, according to Eq. (1),

$$\mathcal{P}=\frac{2g\mu_B}{\beta p}\frac{\partial F_c(M)}{\partial M}. \tag{11}$$

Figure 8 presents the dependence of $\mathcal{P}$ on B_G for the experimentally relevant range of p. We see that $|\mathcal{P}|$ tends to saturate with the increasing $|B_G|$, and thus with M. This means that for large values of the splitting B_G the magnetization M evaluated from the anomalous Hall effect is underestimated. At the same time, the calculation demonstrates that despite the spin-orbit interaction $|\mathcal{P}|$ becomes greater than 0.8 for $3|B_G|>|\varepsilon_F|$. This is due to the fact that the redistribution of the holes over the spin subbands occurs in the way that maximizes the gain of exchange energy, and thus the magnitude of $|\mathcal{P}|$. This is in contrast to the case $|\varepsilon_F|\gg|B_G|$, for which the spin polarization is reduced by a factor greater than 2 from the value corresponding to the absence of spin-orbit coupling at low hole concentrations. We also note that because of the antiferromagnetic character of the p-d coupling ($\beta N_0<0$) the polarization of the hole spins is oriented in the opposite direction to the polarization of the Mn spins.

C. Easy axis and anisotropy field

Early studies of a ferromagnetic phase in (Ga,Mn)As epilayers already demonstrated the existence of substantial magnetic anisotropy.[63] Magnetic anisotropy is usually associated with the interaction between spin and orbital degrees of freedom of the *magnetic* electrons. According to the model in question, these electrons are in the d^5 configuration. For such a case the orbital momentum $L=0$, so that no effects stemming from the spin-orbit coupling are to be expected. To reconcile the model and the experimental observations, we note that the interaction between the localized spins is mediated by the holes, characterized by a nonzero orbital momentum. An important aspect of the present model is that it does take into account the anisotropy of the carrier-mediated exchange interaction associated with the spin-orbit coupling in the host material, an effect difficult to include within the standard approach to the RKKY interaction.

We start by considering an unstrained thin film with the [001] crystal direction perpendicular to its plane. The linear response is isotropic in cubic systems but magnetic anisotropy develops for nonzero magnetization: the hole energy depends on the orientation of M with respect to the crystal axes and, because of stray field energy E_d, on the angle Θ between M and the normal to the film surface. A computation of the hole energies $E_c[M]$ for relevant parameters and [100], [110], and [111] orientations of $\mathbf{M}$ indicates that $E_c[M]$ can be described by the lowest-order cubic anisotropy, so that, taking the stray field energy into account,[64]

$$E_c(M,\Theta,\varphi)-E_c(M,\pi/2,0)$$

$$=K_d(M)\cos^2\Theta+K_{c1}(M)(\sin^4\Theta\sin^2\varphi\cos^2\varphi+\sin^2\Theta\cos^2\Theta), \tag{12}$$

where $K_d(M)=2\pi M^2$. For $4K_d<-K_{c1}$ the easy axis is oriented along [111] or equivalent directions. Otherwise, as is usually the case for parameters of (Ga,Mn)As, $\mathbf{M}$ lies in the (001) plane, and the easy axis is directed along the [100] for $K_{c1}>0$ or along the [110] (or equivalent) crystal axis in the opposite case. It turns out that the sign of K_{c1} depends on the degree of occupation of the hole subbands as well as on their mixing by the p-d and $k\cdot p$ interactions. As a result, the easy axis fluctuates between [100] and [110] as a function of p. To quantify the strength of the cubic anisotropy in (Ga,Mn)As we computed $K_{c1}(M)$, and then the minimum magnitude of an external magnetic field $H_{cu}=2|K_{c1}/M|$ (or $\mu_0 H_{cu}=2|K_{c1}/M|$ in SI units), that aligns the spontaneous magnetization $\mathbf{M}$ along the hard direction. Figure 9 shows how H_{cu}/M and the direction of the easy axis oscillate as a function of p for various $B_G=A_F\beta M/6g\mu_B$. As expected, H_{cu} tends to zero when B_G decreases. Nevertheless, for $|B_G|=40$ meV ($\mu_0 M\approx 85$ mT), $\mu_0 H_{cu}$ up to 0.2 T can be expected. Since, however, the orientation of the easy axis changes rapidly with p and B_G, intrinsic and extrinsic disorder—which leads to broadening of hole subbands—will presumably diminish the actual magnitude of the magnetic anisotropy.

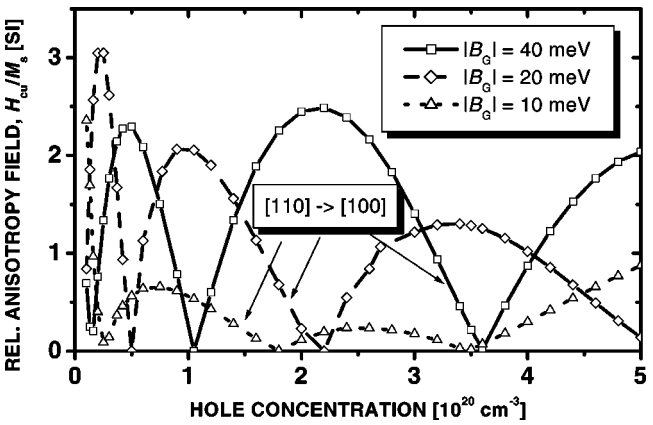

FIG. 9. Computed minimum magnetic field H_{cu} (divided by M) necessary to align magnetization M along the hard axis for cubic (unstrained) $Ga_{1-x}Mn_xAs$ film. As a function of the hole concentration and the spin-splitting parameter B_G, the easy and hard axes fluctuate alternately between [110] and [100] (or equivalent) directions in the plane of the film. The symbol [110] → [100] means that the easy axis is along [110], so that H_{cu} is applied along [100] ($B_G=-30$ meV corresponds to the saturation value of M for $Ga_{0.95}Mn_{0.05}As$).

As shown in Fig. 2, strain has a rather strong influence on the valence subbands. It can therefore be expected that magnetic properties resulting from the hole-mediated exchange can be efficiently controlled by strain engineering. Indeed, sizable lattice-mismatch-driven strain is known to exist in semiconductor layers. In some cases, particularly if epitaxy occurs at appropriately low temperatures, such strain can persist even beyond the critical thickness due to relatively high barriers for the formation of misfit dislocations. We evaluate the magnitude of the resulting effects by using the Bir-Pikus Hamiltonian,[38] adapted for biaxial strain, as shown in Appendix A. Three parameters control strain phenomena in the valence band: the deformation potential b, taken as $b=-1.7$ eV,[65] the ratio of elastic moduli $c_{12}/c_{11}=0.453$,[65] and the difference between the lattice parameters of the substrate and the layer, Δa. The last is related to relevant components of the strain tensor according to

$$\epsilon_{xx}=\epsilon_{yy}=\Delta a/a, \tag{13}$$

$$\epsilon_{zz}=-2\epsilon_{xx}c_{12}/c_{11}. \tag{14}$$

We have found that biaxial strain has a rather small influence on T_C. In the experimentally relevant range of hole concentrations $5\times 10^{20}>p>10^{20}$ cm^{-3}, both tensile and compressive strain diminish T_C. The relative effect attains a maximum at $p\approx 2\times 10^{20}$ cm^{-3}, where $[T_C(\epsilon_{xx})-T_C(0)]/T_C(0)\approx -2.4\%$ and -4.9% for $\epsilon_{xx}=1\%$ and -1%, respectively. However, such a strain leads to uniaxial anisotropy, whose magnitude can be much greater than that resulting from either cubic anisotropy or stray fields. The corresponding anisotropy field H_{un} assumes the form

$$H_{un}=|2\{E_c([001])-E_c([100])\}/M+4\pi M| \text{ (emu)}, \tag{15}$$

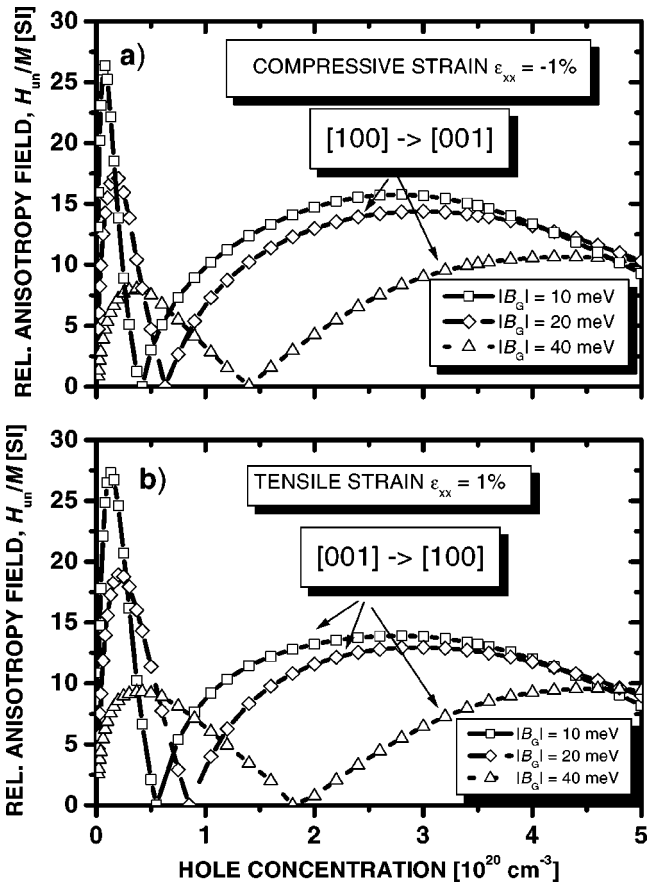

FIG. 10. Computed minimum magnetic field H_{un} (divided by M) necessary to align magnetization M along the hard axis for compressive (a) and tensile (b) biaxial strain in a $Ga_{1-x}Mn_xAs$ film for various values of the spin-splitting parameter B_G. The easy axis is along the [001] direction and in the (001) plane at low and high hole concentrations for compressive strain, respectively (a). The opposite behavior is observed for tensile strain (b). The symbol [100]→[001] means that the easy axis is along [100], so that H_{un} is applied along [001] ($B_G=-30$ meV corresponds to the saturation value of M for $Ga_{0.95}Mn_{0.05}As$).

$$\mu_0 H_{un}=|2\{E_c([001])-E_c([100])\}/M+\mu_0 M| \text{ (SI)}, \tag{16}$$

where the last term describes the stray-field effect. According to the results of computations presented in Fig. 10, in a region of such low hole concentrations that minority spin subbands are depopulated, the easy axis takes the [001] direction for compressive strain, while it is in the (001) plane for the opposite strain. Such a behavior of the magnetic anisotropy was recently noted within a 4×4 model of the valence band.[51] However, for the experimentally relevant hole concentrations and values of B_G (Figs. 10 and 11) the easy axis is oriented along the [001] direction for tensile strain, whereas it resides in the (001) plane for the case of unstrained or compressively strained films. This important result, announced already in our previous work[8] and recently confirmed by others[51] explains the experimental study[63] in which either a (Ga,In)As or GaAs substrate was employed to impose tensile or compressive strain, respectively. In particular, for a $Ga_{0.0965}Mn_{0.035}As$ film on GaAs, for which $\epsilon_{xx}=-0.2\%$, the anisotropy field $\mu_0 H_{un}=0.4\pm0.1$ T is observed,[63] in quantitative agreement with the theoretical results of Fig. 11.

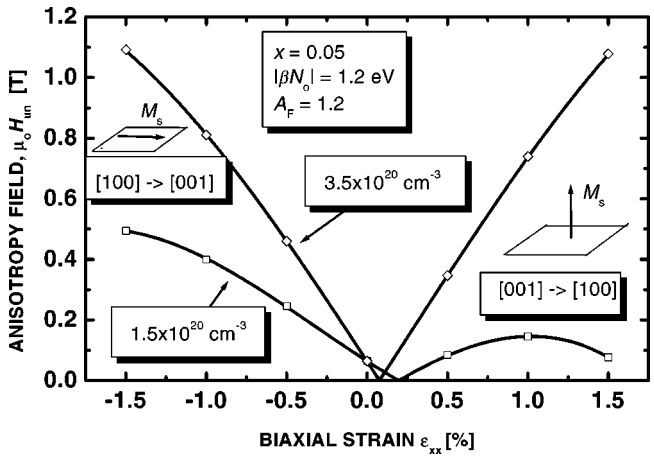

FIG. 11. Computed minimum magnetic field H_{un} necessary to align the saturation value of magnetization M_s along the hard axis as a function of biaxial strain component ϵ_{xx} for two values of the hole concentration in $Ga_{0.95}Mn_{0.05}As$. The symbol [100]→[001] means that the easy axis is along [100], so that H_{un} is applied along [001].

Finally, we mention that strong strain effects may suggest the importance of magnetostriction in the studied compounds. We have not explored this issue yet, and note that prior to its examination the question concerning the collective Jahn-Teller effect in heavily doped p-type zinc-blende semiconductors has to be addressed.

D. Optical absorption and magnetic circular dichroism

In the case of II-VI diluted magnetic semiconductors, detailed information on the exchange-induced spin splitting of the bands, and thus on the coupling between the effective-mass electrons and the localized spins, has been obtained from magneto-optical studies.[26,66] Similar investigations[36,37,67,68] of (Ga,Mn)As led to a number of surprises. The most striking was the opposite order of the absorption edges corresponding to the two circular photon polarizations in (Ga,Mn)As compared to II-VI materials. This behavior of circular magnetic dichroism (MCD) suggests the opposite order of the exchange-split spin subbands, and thus a different origin of the sp-d interaction in these two families of diluted magnetic semiconductors (DMS). Light was shed on the issue by studies of photoluminescence (PL) and its excitation spectra (PLE) in p-type (Cd,Mn)Te quantum wells.[3,53,69] It has been demonstrated that the reversal of the order of PLE edges corresponding to the two circular polarizations results from the Moss-Burstein effect, that is, from the shifts of the absorption edges associated with the empty portion of the valence subbands in the p-type material. This model was subsequently applied to interpret qualitatively the magnetoabsorption data for metallic (Ga,Mn)As.[36] Surprisingly, however, the anomalous sign of the MCD was present also in nonmetallic (Ga,Mn)As, in which an EPR signal from

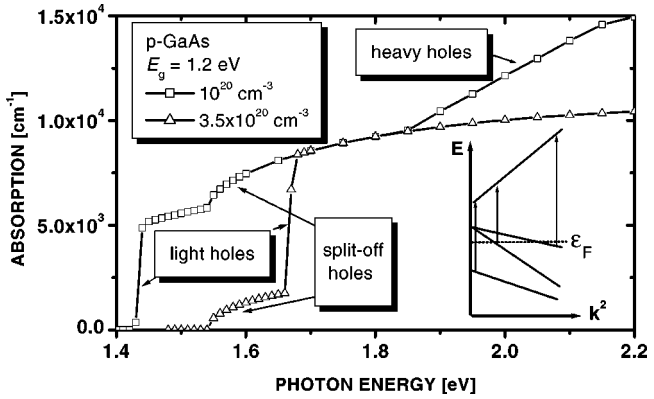

FIG. 12. Absorption edge in p-GaAs computed for two values of the hole concentration. Inset shows three kinds of possible photon-induced transition corresponding to particular valence subbands. Absorption edges associated with electron transitions from particular subbands are labeled.

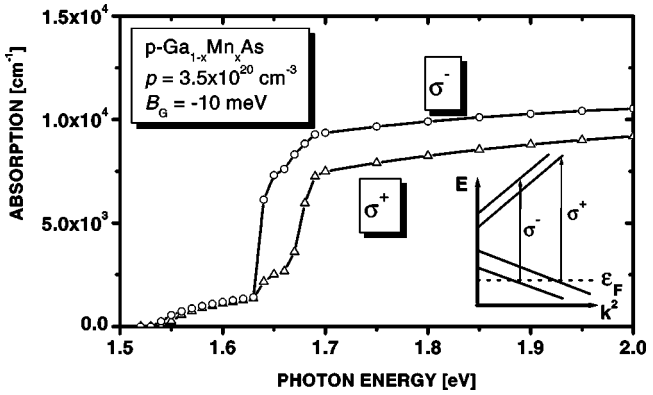

FIG. 13. Absorption edge for two circular polarizations in p-(Ga,Mn)As computed for spin-splitting parameter $B_G=-10$ meV and hole concentration 3.5×10^{20} cm^{-3}. Inset shows how the Fermi sea of the holes reverses relative positions of the edges corresponding to σ^+ and σ^- polarizations. In general, electron transitions from six valence subbands contribute to optical absorption.

occupied Mn acceptors was seen.[35] Another striking property of the MCD is a different temperature dependence of the normalized MCD at low and high photon energies in ferromagnetic (Ga,Mn)As.[37] This observation was taken as evidence for the presence of two spectrally distinct contributions to optical absorption.[37]

We begin by noting that according to our two-fluid model the coexistence of strongly and weakly localized holes is actually expected on both sides of the MIT. Since the Moss-Burstein effect operates for interband optical transitions involving weakly localized states, it leads to a sign reversal of the MCD on the insulating side of the MIT also. Conversely, the existence of the MCD sign reversal can be taken as experimental evidence for the presence of Fermi-liquid-like states on the insulating side of the MIT.

In order to shed some light on these issues we calculate absorption and MCD spectra in a model that takes the complex structure of the valence band into account. The band gap E_g is expected to depend on both Mn and hole concentrations due to the alloy and band-narrowing effects. To take this dependence into account as well as to include disorder-induced band-tail effects[70] we assume, guided by experimental results to be discussed below, that $E_g=1.2$ eV. Our computation of the absorption coefficient $\alpha(\omega)$ is performed according to a scheme outlined in Appendix B, taking the electron effective mass $m_e^*=0.07m_0$, the Kane momentum matrix element $P=9.9\times10^{-8}$ eV cm, and the refractive index $n_r=3.5$. As shown in Fig. 12, contributions to α originating from particular valence bands are clearly visible. Because of the Moss-Burstein shift, the onset and the form of $\alpha(\omega)$ for particular transitions depend on the hole concentration. In particular, $\alpha(\omega)$ corresponding to the light-hole band exhibits a steplike behavior which, in the case of the heavy-hole band, is broadened by warping. While no quantitative data on $\alpha(\omega)$ are available for (Ga,Mn)As, the computed magnitude and spectral dependence of $\alpha(\omega)$ correctly reproduce experimental results for p-GaAs.[71]

The influence of the sp-d band splittings on the absorption edge is shown in Fig. 13. The computation is carried out for the Faraday configuration and with the value of the s-d exchange energy $\alpha N_0=0.2$ eV observed in II-VI semiconductors. The theoretical results confirm that the Moss-Burstein effect accounts for the sign reversal of the magnetic circular dichroism. The energy splitting of the absorption edge depends on ω but its magnitude is similar to that observed experimentally.[36] A detailed comparison requires, on the one hand, experimental information about the absolute values of $\alpha(\omega)$ and, on the other, more careful consideration of band-tailing effects. Furthermore, contributions from intra-valence-band and intra-d-shell transitions are expected at the low- and high-energy wings of the absorption edge, respectively. We predict that not only the former but also the latter will be substantially enlarged in p-type materials. Indeed, the empty valence band states allow for admixtures of p-like states to the localized d orbitals.

The magnetization-induced splitting of the bands is seen to lead to a large energy difference between the positions of the absorption edges corresponding to the two opposite circular polarizations. This may cause an unusual dependence of the low-energy onset of MCD on magnetization, and thus on temperature. In particular, a standard assumption about the proportionality of MCD and magnetization becomes invalid. To find out whether this large splitting is responsible for the anomalous temperature dependence of MCD at low photon energies,[37] we compute the differential transmission coefficient that was examined experimentally,[37]

$$\Delta=(T^+-T^-)/(T^++T^-). \tag{17}$$

Here T^+ and T^- are the transmission coefficients for right and left circularly polarized light. To take the effect of interference into account,[37] these coefficients are calculated for the actual layout of the samples, which consisted of a transparent (Ga,Al)As etching stop layer and the absorbing (Ga,Mn)As film, each 200 nm thick. The same value of the refractive index $n_r=3.5$ is adopted for both compounds.

Figure 14 shows the ratio $\Delta(\omega)/\Delta(1.78\text{ eV})$ computed for $p=3.5\times10^{20}$ cm^{-3} and various $B_G\sim M$. In the range of high photon energies, $\omega>1.6$ eV, the results collapse onto one

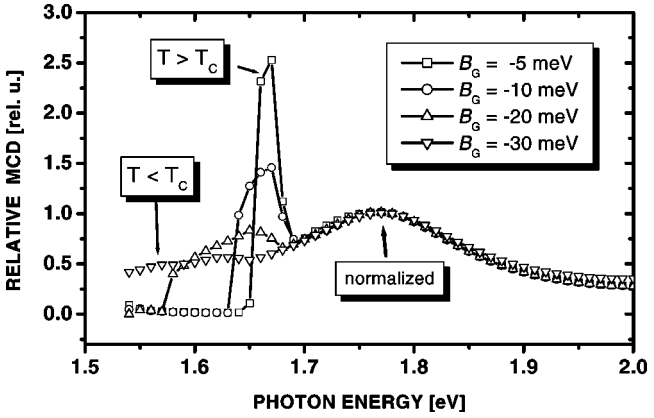

FIG. 14. Spectral dependence of magnetic circular dichroism in p-(Ga,Mn)As computed for hole concentration 3.5×10^{20} cm^{-3} and various spin-splitting parameters B_G. The magnitudes of MCD at a given B_G are normalized by its value at 1.78 eV.

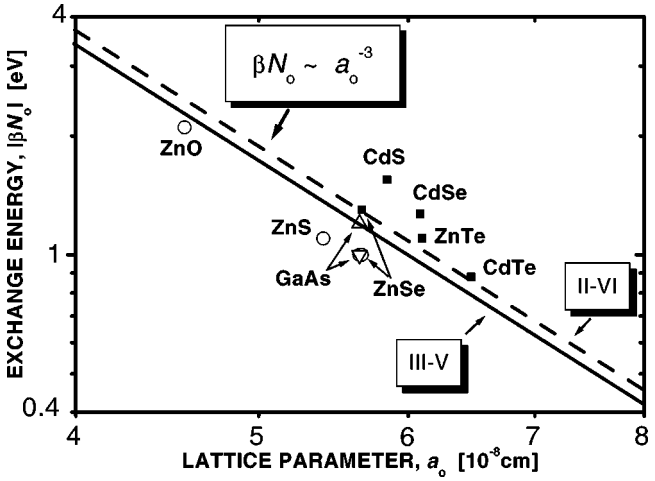

FIG. 15. Energy of p-d exchange interaction for various materials containing 5% of Mn in cation sites as a function of lattice parameter. The values shown by solid squares were determined from excitonic splittings in the magnetic field (Refs. 22, 42, 72, and 79) while the empty symbols denote values evaluated from photoemission data (Refs. 24 and 78). Solid and dashed lines represent formulas adopted for the determination of the exchange energy for other materials, as shown in Tables I and II below.

curve for all values of B_G. This means that $\Delta(\omega)=M(T)f(\omega)$ in this range, where $f(\omega)\sim T^{-1}\partial T/\partial\omega$. However, in the region of the absorption edge, the dependence of Δ on B_G is by no means linear, so that the normalized values $\Delta(\omega)/\Delta(1.78\text{ eV})$ do not follow any single curve. As seen, $\Delta(\omega)/\Delta(1.78\text{ eV})$ peaks at a larger value for smaller B_G. This is the behavior found experimentally.[37] We conclude that the two observed distinct spectroscopic regions[37] correspond to standard band-to-band transitions, for which the proportionality of Δ to B_G holds, and to the onset of the absorption edge, which is shifted and made steeper by the Moss-Burstein effect. Actually, the peak values of $\Delta(\omega)/\Delta(1.78\text{ eV})$ determined numerically for the low-energy region are even greater than that observed in (Ga,Mn)As,[37] presumably because of scattering broadening of the absorption edge, neglected in our model.

V. CHEMICAL TRENDS

A. Material parameters

The ability of the present model to describe successfully various aspects of the ferromagnetism in (Ga,Mn)As, as well as in (Zn,Mn)Te,[4,8,43] has encouraged us to extend the theory toward other p-type diluted magnetic semiconductors. In this section, we present material parameters that have been adopted for the computations presented elsewhere.[8] We also supplement the previous results[8] by the data for (In,Mn)N, (Zn,Mn)S, (Cd,Mn)S, and (Cd,Mn)Se. Along with Si and Ge,[8] we take into consideration here carbon in the diamond structure. For concreteness, we will assume that 5% of the cation sites (i.e., 2.5% of atom sites) are occupied by Mn ions in the d^5 2+ charge state, and that the corresponding localized spins $S=\frac{5}{2}$ are coupled by the indirect exchange interaction mediated by 3.5×10^{20} holes per cm^3. The enhancement effect of the exchange interaction among the holes is described by the Fermi-liquid parameter $A_F=1.2$. As explained in Sec. II B, no influence of the antiferromagnetic superexchange is taken into account in the case of the groups III-V and IV semiconductors, in which the Mn supplies both localized spins and holes. By contrast, it is assumed that in the case of II-VI semiconductors $x_{\text{eff}}=0.0297$ for $x=0.05$ and $T_{\text{AF}}=1$ K, except for (Zn,Mn)Te, where $T_{\text{AF}}=2.9$ K,[41,42] and (Cd,Mn)Te, for which $T_{\text{AF}}=1.5$ K.[72]

The values of the parameters that are used to determined chemical trends are summarized in Appendix C, Tables I and II, for cubic and wurzite semiconductors, respectively. If no experimentally determined values are available, the effective-mass parameters are determined by fitting the appropriate $k\cdot p$ model to results of band structure computations. No lattice polaron corrections are taken into consideration. Since we are interested in a relatively small concentration of magnetic ions, $x=0.05$, the effect of the Mn incorporation upon the lattice and band structure parameters is disregarded.

In the case of ZnSe, the recently determined[73,74] values of the Luttinger parameters γ_i lead to a negative hole mass for the [110] crystallographic direction, an effect not supported by the existing theoretical studies of the valence band structure in this material.[75,76] Accordingly, an older set[77] of γ_i had been taken for the previous calculation.[8] The present values of γ_i are within experimental uncertainties of the current determinations[73] and, at the same time, lead to a good description of the computed band structure of the valence band in ZnSe.[75]

In addition to the spin density of states at the Fermi level, the Curie temperature is proportional to the square of the p-d exchange integral β. Figure 15 presents the magnitudes of the exchange energy βN_0 as determined by photoemission and magneto-optical studies for various DMS containing about 5% of Mn. The values of $|\beta N_0|$ are seen to increase when the lattice parameter decreases. This trend stems[78] from the corresponding changes in the charge-transfer and correlation energies as well as from a dependence of the p-d hybridization energy on the bond length b.[78] It should, how-

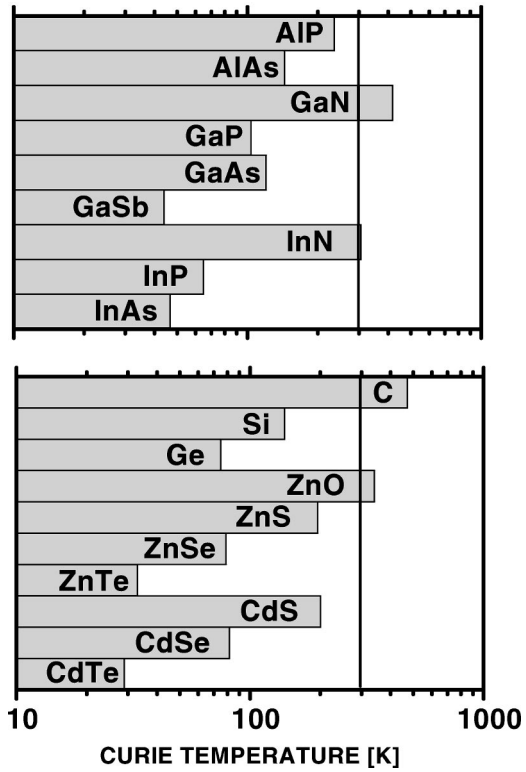

FIG. 16. Curie temperatures evaluated for various III-V (top panel) as well group IV and II-VI semiconducting compounds (lower panel) containing 5% of Mn per cation (or 2.5% per atom) in 2+ charge state and 3.5×10^{20} holes per cm^3. Material parameters adopted for the calculation are displayed in Appendix C, Tables I and II.

ever, be recalled that *b*, in contrast to the average value of the lattice constant, does not obey the Vegard law in alloys but rather conserves the value corresponding to the end compounds.[13]

Thus, in order to obtain the values of βN_0 for materials for which no direct determination is available, guided by the results presented in Fig. 15, we assume $\beta N_0 \sim a_0^{-3}$, i.e., β = const. More explicitly, for groups III-V and IV semiconductors we take

$$\beta_{\text{III-V}} = \beta(\text{GaMnAs}). \tag{18}$$

Similarly, for the II-VI materials,

$$\beta_{\text{II-VI}} = \beta(\text{ZnMnSe}), \tag{19}$$

where the p-d energy $\beta N_0(\text{GaMnAs}) = -1.2$ eV,[24] and $\beta N_0(\text{ZnMnSe}) = -1.3$ eV.[79]

B. Curie temperatures

Figure 16 presents the calculated values of the Curie temperature T_C for III-V and II-VI semiconductors containing 5% of Mn in the cation sublattice and 3.5×10^{20} holes per cm^3. It has been assumed that the Mn remains in the d^5 configuration in all compounds, although it seems that other situations are possible, such as the d^4 configuration of Mn in GaP.[80] The data for diamond structure C, Si, and Ge with 2.5% of Mn in the 2^+ charge state and occupying substitutional sites are also included. The most remarkable result is a strong increase of T_C for materials consisting of lighter elements. In fact, T_C exceeding room temperature is expected for C, GaN, InN, and ZnO for the assumed values of the Mn and hole concentrations. It has been checked for GaN that the value of T_C for the zinc-blende modification of this material is greater by 6% than that for the wurzite case.

By comparing results of numerical calculations with the general Eq. (7) for T_C three interrelated mechanisms accounting for the chemical trends visible in Fig. 16 can be identified. First, the reduction of the spin density of states and thus T_C by the spin-orbit interaction ceases to operate in materials with light anions. Second, the effective mass and thus the density of states tend to increase for materials with stronger bonds. Finally, a smaller lattice constant at given *x* corresponds to the greater value of $N_0 x$, the density of the magnetic ions. It should be noted at this point that T_C is proportional to β^2, assumed here to be material independent. This assumption corresponds, however, to a strong increase of $|\beta N_0|$ with decreasing lattice constant, as shown in Fig. 15.

It can be expected that the chemical trends established here will not be altered by the uncertainties in the values of the relevant parameters. Our evaluation of the strength of the ferromagnetic interactions mediated by the holes is qualitatively valid for Mn, as well as for other magnetic ions, provided that two conditions are met. First, the magnetic electrons stay localized and do not contribute directly to the Fermi sphere. Secondly, the holes are delocalized and, in particular, do not form small magnetic polarons, such as Zhang-Rice singlets.[21]

VI. SUMMARY AND OUTLOOK

In this paper, a theory of ferromagnetism in *p*-type zinc-blende and wurzite semiconductors containing a sizable concentration of magnetic ions has been proposed. It has been argued that over the relevant range of hole densities the ferromagnetic coupling between the localized spins is primarily mediated by delocalized or weakly localized holes residing in a p-like valence band. Accordingly, particular attention has been paid to incorporating into the Zener model the effects of $k\cdot p$ and spin-orbit interactions as well as of biaxial strain. It has been assumed that, like other thermodynamic properties of doped semiconductors, the Curie temperature is not affected by disorder, despite the proximity to the metal-insulator transition. The effects of the carrier-carrier interactions have been taken into account by a density-independent Landau renormalization of the carrier spin susceptibility. It has been demonstrated that the theory describes qualitatively, and often quantitatively, a body of experimental results accumulated over recent years for (Ga,Mn)As. In particular, the Curie temperature, the saturation value of the magnetization, the hole spin magnetization and polarization, magnetic anisotropies and magnetoelastic effects, optical absorption, and magnetic circular dichroism have been interpreted.

Giant negative magnetoresistance, a sharp field-induced

insulator-to-metal transition,[81] and a sizable increase of high-frequency conductivity with increasing magnetic field[82] were observed in *p*-(Hg,Mn)Te. Those findings were attributed to the growing participation of the light holes in transport when the p-d exchange splitting increases.[81,82] This implies a shift of the Drude weight from high to low frequencies as a function of the valence band splitting. Such effects in both dc (Refs. 14 and 83) and ac (Refs. 84 and 85) conductivity have more recently been detected in (Ga,Mn)As, and can qualitatively be interpreted in the same way. This provides additional support for our conclusion about the similarity of the mechanisms accounting for the hole-mediated exchange interaction in II-VI and III-V magnetic semiconductors. However, our work identifies also an aspect of ferromagnetism, that points to a difference between these two families of magnetic semiconductors. In the case of II-VI compounds, a short-range antiferromagnetic superexchange lowers the magnitude of T_C. This lowering appears to be much less efficient in III-V semiconductors, where the Mn ions act as acceptors, compensated partly by donor defects. Thus, the localized holes reside preferentially on the Mn pairs, so that the hole-mediated ferromagnetic coupling (a variant of Zener's double exchange) can overcompensate the antiferromagnetic superexchange. Accordingly, the calculations for the III-V compounds have been carried out assuming $x_{\mathrm{eff}}=0$ and $T_{\mathrm{AF}}=0$.

The model put forward here has also been used to explore the expected chemical trends. It was found that particularly large values of the Curie temperature are expected for materials built up from light elements. However, important issues of solubility limits and self-compensation need to be addressed experimentally. In particular, the pinning of the Fermi energy by *AX*-type centers or other defects can preclude an increase of hole concentration in many systems. High-pressure research can shed some light on this issue. Since, in general, III-V compounds can be more easily be doped by impurities that are electrically active, whereas a large quantity of transition metals can be incorporated into II-VI materials, the suggestion has been put forward to grow magnetic III-V/II-VI short-period superlattices.[86] Further numerical and experimental studies of magnetic semiconductors as well as of heavily *p*-doped nonmagnetic systems are expected to improve our understanding of the hole-mediated ferromagnetism in zinc-blende and wurzite compounds. This, together with exploration of quantum structures as well as of codoping and coalloying, may lead to fabrication of functional systems.

On the theoretical side, further work is necessary to evaluate quantitative corrections to the mean-field theory brought about by thermodynamic fluctuations of magnetization. Effects of disorder associated with both random distribution of magnetic ions and fluctuations of carrier density near the metal-insulator transition are other open issues. In particular, the nature of the evolution of static and dynamic magnetic phenomena on approaching the strongly localized regime is unknown. In this range, description of the effect of the carrier-carrier interaction in terms of the Landau theory of Fermi liquids may break down. The above list of interesting problems is by no means exhaustive. No doubt we will soon witness many unforeseen developments in the field of carrier-mediated ferromagnetism in semiconductors.

ACKNOWLEDGMENTS

The work at Tohoku University was supported by the Japan Society for the Promotion of Science and by the Ministry of Education, Japan; the work in Poland by the State Committee for Scientific Research, Grant No. 2-P03B-02417, and by the Foundation for Polish Science.

APPENDIX A: EFFECTIVE-MASS HAMILTONIANS

The purpose of this Appendix is to provide the explicit form of the effective-mass Hamiltonian that, in addition to the standard $k\cdot p$ and strain terms,[38] contains a contribution of the p-d exchange interaction in the molecular-field approximation. This is a generalization of previous approaches[39,66] by allowing for arbitrary orientation of the magnetization *M* with respect to the crystal axes.

Zinc-blende semiconductors are considered first. We take into account explicitly four Γ_8 and two Γ_7 valence subbands, for which we choose the basis functions in the form

$$u_1=\frac{1}{\sqrt{2}}(X+iY)\uparrow, \tag{A1}$$

$$u_2=i\frac{1}{\sqrt{6}}[(X+iY)\downarrow-2Z\uparrow], \tag{A2}$$

$$u_3=\frac{1}{\sqrt{6}}[(X-iY)\uparrow+2Z\downarrow], \tag{A3}$$

$$u_4=i\frac{1}{\sqrt{2}}(X-iY)\downarrow, \tag{A4}$$

$$u_5=\frac{1}{\sqrt{3}}[(X+iY)\downarrow+Z\uparrow], \tag{A5}$$

$$u_6=i\frac{1}{\sqrt{3}}[-(X-iY)\uparrow+Z\downarrow], \tag{A6}$$

where *X*, *Y*, and *Z* denote Kohn-Luttinger amplitudes, which for the symmetry operations of the crystal point group transform as p_x, p_y, and p_z wave functions of the hydrogen atom.

In the above basis the corresponding Luttinger-Kohn matrices assume the following forms.

1. $k\cdot p$ matrix

$$H_{k\cdot p}=-\frac{\hbar^2}{2m_0}\begin{bmatrix} P+Q & L & M & 0 & iL/\sqrt{2} & -i\sqrt{2}M \\ L^* & P-Q & 0 & M & -i\sqrt{2}Q & i\sqrt{3/2}L \\ M^* & 0 & P-Q & -L & -i\sqrt{3/2}L^* & -i\sqrt{2}Q \\ 0 & M^* & -L^* & P+Q & -i\sqrt{2}M^* & -iL^*/\sqrt{2} \\ -iL^*/\sqrt{2} & i\sqrt{2}Q & i\sqrt{3/2}L & i\sqrt{2}M & P+\Delta & 0 \\ i\sqrt{2}M^* & -i\sqrt{3/2}L^* & i\sqrt{2}Q & iL/\sqrt{2} & 0 & P+\Delta \end{bmatrix}. \tag{A7}$$

Here,

$$P=\gamma_1 k^2, \tag{A8}$$

$$Q=\gamma_2(k_x^2+k_y^2-2k_z^2), \tag{A9}$$

$$L=-i2\sqrt{3}\gamma_3(k_x-ik_y)k_z, \tag{A10}$$

$$M=\sqrt{3}[\gamma_2(k_x^2-k_y^2)-i2\gamma_3 k_x k_y], \tag{A11}$$

$$\Delta=2m_0\Delta_0/\hbar^2. \tag{A12}$$

2. p-d exchange matrix

$$H_{\mathrm{pd}}=B_G\begin{bmatrix} 3b_x w_z & i\sqrt{3}b_x w_- & 0 & 0 & \sqrt{6}b_x w_- & 0 \\ -i\sqrt{3}b_x w_+ & (2b_z-b_x)w_z & 2ib_z w_- & 0 & i\sqrt{2}(b_x+b_z)w_z & -\sqrt{2}b_z w_- \\ 0 & -2ib_z w_+ & -(2b_z-b_x)w_z & i\sqrt{3}b_x w_- & \sqrt{2}b_z w_+ & -i\sqrt{2}(b_x+b_z)w_z \\ 0 & 0 & -i\sqrt{3}b_x w_+ & -3b_x w_z & 0 & -\sqrt{6}b_x w_+ \\ \sqrt{6}b_x w_+ & -i\sqrt{2}(b_x+b_z)w_z & \sqrt{2}b_z w_- & 0 & -(2b_x-b_z)w_z & ib_z w_- \\ 0 & -\sqrt{2}b_z w_+ & i\sqrt{2}(b_x+b_z)w_z & -\sqrt{6}b_x w_- & -ib_z w_+ & (2b_x-b_z)w_z \end{bmatrix}. \tag{A13}$$

Here,

$$B_G=\beta M/6g\mu_B, \tag{A14}$$

$$w_z=M_z/M, \tag{A15}$$

$$w_\pm=(M_x\pm iM_y)/M, \tag{A16}$$

$$b_z=\beta_z/\beta, \tag{A17}$$

$$b_x=\beta_x/\beta, \tag{A18}$$

where in cubic materials $b_z=b_x=1$.

3. Biaxial strain matrix

$$H_{\mathrm{BS}}=b\begin{bmatrix} -Q_\epsilon & 0 & R_\epsilon & 0 & 0 & -i\sqrt{2}R_\epsilon \\ 0 & Q_\epsilon & 0 & R_\epsilon & i\sqrt{2}Q_\epsilon & 0 \\ R_\epsilon & 0 & Q_\epsilon & 0 & 0 & i\sqrt{2}Q_\epsilon \\ 0 & R_\epsilon & 0 & -Q_\epsilon & -i\sqrt{2}R_\epsilon & 0 \\ 0 & -i\sqrt{2}Q_\epsilon & 0 & i\sqrt{2}R_\epsilon & 0 & 0 \\ i\sqrt{2}R_\epsilon & 0 & -i\sqrt{2}Q_\epsilon & 0 & 0 & 0 \end{bmatrix}. \tag{A19}$$

Here, b is the deformation potential and

$$Q_\epsilon = \epsilon_{zz} - (\epsilon_{xx} + \epsilon_{yy})/2, \tag{A20}$$

$$R_\epsilon = \sqrt{3}(\epsilon_{xx} - \epsilon_{yy})/2. \tag{A21}$$

Since we are interested in the effect of the biaxial strain in the (001) plane, only the terms involving the diagonal components ϵ_{ii} of the deformation tensor are included. For the same reason, we allow for the corresponding anisotropy of the exchange integrals $\beta_x = \beta_y \neq \beta_z$, although we expect that to a good accuracy $\beta_x = \beta_z$ in real systems. The latter is assumed in the main body of the paper.

In the presence of the magnetic field B the Luttinger-Kohn $k \cdot p$ matrix is a sum of the Zeeman and Landau parts, $H_{k\cdot p} = H_Z + H_L$, where H_L is written below for $\mathbf{B} \| [001]$ and neglecting some terms proportional to $\gamma_2 - \gamma_3$.[87]

$$H_Z = -g_0 \mu_B B \begin{bmatrix} 3\kappa w_z/2 & i\sqrt{3}\kappa w_-/2 & 0 & \cdots \\ -i\sqrt{3}\kappa w_+/2 & \kappa w_z/2 & i\kappa w_- & \cdots \\ 0 & -i\kappa w_+ & -\kappa w_z/2 & \cdots \\ 0 & 0 & -i\sqrt{3}\kappa w_+/2 & \cdots \\ -\sqrt{6}(\kappa+1)w_+/4 & i\sqrt{2}(\kappa+1)w_z/2 & -\sqrt{2}(\kappa+1)w_-/4 & \cdots \\ 0 & \sqrt{2}(\kappa+1)w_+/4 & -i\sqrt{2}(\kappa+1)w_z/2 & \cdots \end{bmatrix}$$
$$\times \begin{bmatrix} 0 & -\sqrt{6}(\kappa+1)w_-/4 & 0 \\ 0 & -i\sqrt{2}(\kappa+1)w_z/2 & \sqrt{2}(\kappa+1)w_-/4 \\ i\sqrt{3}\kappa w_-/2 & -\sqrt{2}(\kappa+1)w_+/4 & i\sqrt{2}(\kappa+1)w_z/2 \\ -3\kappa w_z/2 & 0 & \sqrt{6}(\kappa+1)w_+/4 \\ 0 & (\kappa+1/2)w_z & -i(\kappa+1/2)w_- \\ \sqrt{6}(\kappa+1)w_-/4 & i(\kappa+1/2)w_+ & -(\kappa+1/2)w_z \end{bmatrix}, \tag{A22}$$

where g_0 is the Landé factor of the free electron, and

$$w_z = B_z/B, \tag{A23}$$

$$w_\pm = B_x \pm iB_y. \tag{A24}$$

For the Landau quantum number $n > 0$,

$$H_L = -\frac{\hbar^2}{2m_0} \begin{bmatrix} h_h + s(\gamma_1+\gamma_2)(2n-1) & b\sqrt{n} & c\sqrt{n(n+1)} & \cdots \\ -b\sqrt{n}h_l + s(\gamma_1-\gamma_2)(2n+1) & 0 & c\sqrt{(n+1)(n+2)} & \cdots \\ c\sqrt{n(n+1)} & 0 & h_l + s(\gamma_1-\gamma_2)(2n+3) & \cdots \\ 0 & c\sqrt{(n+1)(n+2)} & b\sqrt{n+2} & \cdots \\ ib\sqrt{n/2} & iq + i\sqrt{2}\gamma_2 s(2n+1) & ib\sqrt{3(n+1)/2} & \cdots \\ ic\sqrt{2(n+1)n} & ib\sqrt{3(n+1)/2} & iq + i\sqrt{2}\gamma_2 s(2n+3) & \cdots \end{bmatrix}$$
$$\times \begin{bmatrix} 0 & ib\sqrt{n/2} & -ic\sqrt{2n(n+1)} \\ -iq - i\sqrt{2}s\gamma_2(2n+1) & ib\sqrt{3(n+1)/2} & \\ -b\sqrt{(n+2)} & ib\sqrt{3(n+1)/2} & -iq - i\sqrt{2}\gamma_2 s(2n+3) \\ h_h + (\gamma_1+\gamma_2)s(2n+5) & -ic\sqrt{2(n+1)(n+2)} & ib\sqrt{(n+2)/2} \\ ic\sqrt{2(n+2)(n+1)} & h_s + \gamma_1 s(2n+1) & 0 \\ ib\sqrt{(n+2)/2} & 0 & h_s + \gamma_1 s(2n+3) \end{bmatrix}. \tag{A25}$$

Here,

$$s = eB/\hbar, \tag{A26}$$

$$h_h = (\gamma_1 - 2\gamma_2)k_z^2, \tag{A27}$$

$$h_l = (\gamma_1 + 2\gamma_2)k_z^2, \tag{A28}$$

$$h_s = \gamma_1 k_z^2, \tag{A29}$$

$$q = -2\sqrt{2}\gamma_2 k_z^2, \tag{A30}$$

$$b = -i2\sqrt{6s}\gamma_3 k_z, \tag{A31}$$

$$c = \sqrt{3}s(\gamma_2 + \gamma_3). \tag{A32}$$

If $n=0$, the wave-function basis does not contain the u_1 term, so that

$$H_L = -\frac{\hbar^2}{2m_0}\begin{bmatrix} h_l + s(\gamma_1-\gamma_2)(2n+1) & 0 & \sqrt{(n+2)(n+1)} & \cdots \\ 0 & h_l + s(\gamma_1-\gamma_2)(2n+3) & -b\sqrt{n+2} & \cdots \\ c\sqrt{(n+2)(n+1)} & b\sqrt{n+2} & h_h + (\gamma_1+\gamma_2)s(2n+5) & \cdots \\ iq + i\sqrt{2}\gamma_2 s(2n+1) & ib\sqrt{3(n+1)/2} & ic\sqrt{2(n+2)(n+1)} & \cdots \\ ib\sqrt{3(n+1)/2} & iq + i\sqrt{2}\gamma_2 s(2n+3) & ib\sqrt{(n+2)/2} & \cdots \end{bmatrix}$$

$$\times \begin{bmatrix} -iq - i\sqrt{2}s\gamma_2(2n+1) & ib\sqrt{3(n+1)/2} \\ ib\sqrt{3(n+1)/2} & -iq - i\sqrt{2}\gamma_2 s(2n+3) \\ -ic\sqrt{2(n+2)(n+1)} & ib\sqrt{(n+2)/2} \\ h_s + \gamma_1 s(2n+1) & 0 \\ 0 & h_s + \gamma_1 s(2n+3) \end{bmatrix}. \tag{A33}$$

If $n=-1$, the wave-function basis does not contain the u_1, u_2, and u_5 terms, so that

$$H_L = -\frac{\hbar^2}{2m_0}\begin{bmatrix} h_l + s(\gamma_1-\gamma_2)(2n+3) & -b\sqrt{n+2} & -iq - i\sqrt{2}\gamma_2 s(2n+3) \\ b\sqrt{n+2} & h_h + (\gamma_1+\gamma_2)s(2n+5) & ib\sqrt{(n+2)/2} \\ iq + i\sqrt{2}\gamma_2 s(2n+3) & ib\sqrt{(n+2)/2} & h_s + \gamma_1 s(2n+3) \end{bmatrix}. \tag{A34}$$

If $n=$-2, the wave-function basis contains only the u_4 term, so that

$$H_L = -\frac{\hbar^2}{2m_0}[h_h + (\gamma_1+\gamma_2)s]. \tag{A35}$$

The solution of the eigenvalue and eigenfunction problem for the Hamiltonian $H = H_{k\cdot p} + H_{pd} + H_{\mathrm{BS}}$ or, in the magnetic field, $H = H_L + H_Z + H_{pd} + H_{\mathrm{BS}}$ gives the hole energies ε_i and eigenvectors $a_i^{(j)}$ for the six relevant hole subbands.

4. Wurzite compounds

For wurzite compounds, we chose the basis in the form

$$u_1 = -\frac{1}{\sqrt{2}}(X+iY)\uparrow, \tag{A36}$$

$$u_2 = \frac{1}{\sqrt{2}}(X-iY)\uparrow, \tag{A37}$$

$$u_3 = Z\uparrow, \tag{A38}$$

$$u_4 = \frac{1}{\sqrt{2}}(X-iY)\downarrow, \tag{A39}$$

$$u_5 = -\frac{1}{\sqrt{2}}(X+iY)\downarrow \tag{A40}$$

$$u_6 = Z\downarrow. \tag{A41}$$

In the above basis, the $k\cdot p$ matrix reads

$$\frac{\hbar^2}{2m_0}\begin{bmatrix} F & -K^* & -H^* & 0 & 0 & 0 \\ -K & F-2\Delta_2 & H & 0 & 0 & \sqrt{2}\Delta_3 \\ -H & H^* & L-\Delta_1-\Delta_2 & 0 & \sqrt{2}\Delta_3 & 0 \\ 0 & 0 & 0 & F & -K & H \\ 0 & 0 & \sqrt{2}\Delta_3 & -K^* & F-2\Delta_2 & -H^* \\ 0 & \sqrt{2}\Delta_3 & 0 & H^* & -H & L-\Delta_1-\Delta_2 \end{bmatrix}. \tag{A42}$$

Here,

$$L=A_1k_z^2+A_2(k_x^2+k_y^2), \tag{A43}$$

$$T=A_3k_z^2+A_4(k_x^2+k_y^2), \tag{A44}$$

$$F=L+T, \tag{A45}$$

$$k_+=k_x+ik_y, \tag{A46}$$

$$K=A_5k_+^2, \tag{A47}$$

$$H=A_6k_+k_z, \tag{A48}$$

where Δ_i and A_i are the valence band splittings and $k\cdot p$ parameters, respectively.

The p-d exchange matrix is given by

$$H_{\mathrm{pd}} = 3B_G\begin{bmatrix} b_xw_z & 0 & 0 & 0 & b_xw_m & 0 \\ 0 & b_xw_z & 0 & b_xw_m & 0 & 0 \\ 0 & 0 & b_zw_z & 0 & 0 & b_zw_m \\ 0 & b_xw_p & 0 & -b_xw_z & 0 & 0 \\ b_xw_p & 0 & 0 & 0 & -b_xw_z & 0 \\ 0 & 0 & b_zw_p & 0 & 0 & -b_zw_z \end{bmatrix}. \tag{A49}$$

APPENDIX B: NUMERICAL PROCEDURE

We aim at evaluating the Helmholtz free energy F_c at given hole concentration p as a function of the Mn magnetization M,

$$F_c(p,M)=-k_BT\int \mathrm{d}\varepsilon\, N(\varepsilon)\ln(1+\exp\{-[\varepsilon(M) - \varepsilon_F(p,M)]/k_BT\})+p\varepsilon_F(p,M), \tag{B1}$$

where the thermodynamic density of states $N(\varepsilon)=\partial p/\partial\varepsilon$. If $T<200$ K then in the cases studied the hole liquid is degenerate, so that F_c assumes the simple form

$$F_c(p,M)=\int_0^p dp'\,\varepsilon(M,p'). \tag{B2}$$

Thus, in order to obtain $F_c(p,M)$ we have to integrate the dependence of the partition function or of the Fermi energy on the hole concentration for various M. The actual calculation proceeds in a standard way. First, the length of the wave vectors $k_i(\theta,\varphi)$ for each of the six hole subbands is determined by solving the inverse eigenvalue problem for given values of ε, polar angle θ, and azimuth angle φ in the **k**-vector space. Then the hole concentration is obtained by integration of $\Sigma_i k_i^3(\theta,\varphi)/24\pi^3$ over $\cos\theta$ and φ.

In order to calculate the contribution M_c of the hole magnetic moments to the total magnetization, the eigenvalue problem is solved directly, making it possible to determine the Gibbs thermodynamic potential G_c,

$$G_c=-\sum_{i,n,k_z} k_BT(eB/2\pi\hbar)\ln(1+\exp\{-[\varepsilon_i(n,k_z,M) - \varepsilon_F]/k_BT\}). \tag{B3}$$

We calculate the absorption coefficient α for the two circular polarizations $\sigma^{\pm}$, taking into account k-conserving electron transitions from the six valence subbands, index i, to the two spin branches of the conduction band, index j, assuming that the hole liquid is strongly degenerate. In such a model,[88,89]

$$\alpha^{\pm}=\frac{4\pi^2e^2P^2}{\hbar^2cn_r\omega}\sum_{i,j}\int_{-1}^{1}d\cos\theta \times\int_0^{2\pi}d\varphi\frac{k_{ij}(\omega)m_r^{(ij)}(\omega)}{8\pi^3\hbar^2}|M_{ij}^{\pm}|^2. \tag{B4}$$

The wave vectors $k_{ij}(\omega,\theta,\varphi)$ corresponding to 12 possible transitions are determined by energy conservation and the position of the Fermi level. The joint density of states effective mass corresponding to these k_{ij} is given by

$$m_r^{(ij)}=\left(1/m_e-\frac{1}{\hbar^2k_{ij}}\frac{\partial\varepsilon_i}{\partial k_{ij}}\right)^{-1}. \tag{B5}$$

The matrix elements $M_{ij}^{\pm}(\theta,\varphi)$ for the two light polarizations and involving electron transitions to the spin-down and spin-up conduction subbands are given by

$$M_{i1}^{+}=a_i^{(4)}, \tag{B6}$$

$$M_{i2}^{+}=a_i^{(3)}/\sqrt{3}+ia_i^{(6)}\sqrt{2/3}, \tag{B7}$$

$$M_{i1}^{-}=a_i^{(2)}/\sqrt{3}-ia_i^{(5)}\sqrt{2/3}, \tag{B8}$$

$$M_{i2}^{-}=a_i^{(1)}, \tag{B9}$$

where a_i^n is the nth component of the eigenvector corresponding to the ith valence subband at $k_{ij}(\theta,\varphi)$.

APPENDIX C: MATERIAL PARAMETERS

In Tables I and II we summarize band structure parameters of parent compounds employed for the evaluation of chemical trends in cubic and wurzite magnetic semiconductors.

TABLE I. Material parameters of selected cubic semiconductors and the values of the p-d exchange energy βN_0. Except for the parameters for which references are provided, the values of the lattice constant a_0, spin-orbit splitting Δ_0, and Luttinger parameters γ_i are taken from Refs. 65, 76, 90, and 91.

	a_0 (Å)	Δ_0 (eV)	γ_1	γ_2	γ_3	βN_0 (eV)
C	3.56	0.013[a]	2.54[a]	−0.10[a]	0.63[a]	−4.8[b]
Si	5.43	0.044	4.285	0.339	1.446	−1.35[b]
Ge	5.66	0.29	13.38	4.24	5.69	−1.20[b]
AlP	5.47	0.1	3.47	0.06	1.15	−1.33[b]
AlAs	5.66	0.275	3.25	0.64	1.21	−1.19[b]
GaN	4.50[c]	0.018[c]	2.463[d]	0.647[d]	0.975[d]	−2.37[b]
GaP	5.45	0.080	4.05	0.49	1.25	−1.34[b]
GaAs	5.65	0.34	6.85	2.1	2.9	−1.2[e]
GaSb	6.09	0.76	13.3	4.4	5.7	−0.96[b]
InP	5.87	0.108	5.15	0.94	1.62	−1.07[b]
InAs	6.06	0.38	20.4	8.3	9.1	−0.98[b]
ZnS	5.401	0.070	1.77[f]	0.30[f]	0.62[f]	−1.5[g]
ZnSe	5.67	0.43	2.95[h]	0.6[h]	1.11[h]	−1.3[i]
ZnTe	6.10	0.91	3.8	0.72	1.3	−1.1[j]
CdTe	6.48	0.95	4.14	1.09	1.62	−0.88[k]

[a]M. Willazen, M. Cardona, and N. E. Christensen, Phys. Rev. B **50**, 18 054 (1994).
[b]Determined from Eq. (18).
[c]Determined from the data for the wurzite structure (Table II).
[d]Reference 92(a); in this paper the Dresselhaus parameters L,M,N are denoted as A,B,C, respectively; see also I. Stolpe, N. Puhlmann, H.-U. Müller, O. Portugall, M. von Ortenberg, D. Schikora, D. J. As, B. Schöttker, and R. Lischka, Physica B **256-258**, 659 (1998).
[e]From photoemission (Ref. 24).
[f]From theoretical studies (Ref. 75).
[g]Determined from Eq. (19).
[h]Determinations of these values is discussed in the main body of the text.
[i]From magnetoreflectivity (Ref. 79).
[j]From magnetoreflectivity (Ref. 42).
[k]From magnetoreflectivity (Ref. 72).

TABLE II. Material parameters of selected wurzite semiconductors. The values of the lattice parameter $a_0=(\sqrt{3}a^2c)^{1/3}$ and the splittings Δ_i of the valence band at the Γ point in II-VI compounds are taken from Refs.76 and 90. Theoretical studies provide the parameters Δ_i and A_i for GaN (Ref. 92) InN (Ref. 93), and A_i for ZnO, CdS, and CdSe (Ref. 75).

Material	GaN	InN	ZnO	CdS	CdSe
a_0 (Å)	4.503	4.974	4.567	5.845	6.078
Δ_1 (eV)	0.0036	0.017	0.04	0.030	0.039
Δ_2 (eV)	0.005	0.001	0.0	0.022	0.139
Δ_3 (eV)	0.0059	0.001	0.0	0.022	0.139
A_1	−6.4	−9.28	−2.41	−5.92	−10.2
A_2	−0.5	−0.6	−0.44	−0.70	−0.76
A_3	5.9	8.68	2.11	5.37	9.53
A_4	−2.55	−4.34	−1.06	−1.82	−3.2
A_5	−2.56	−4.32	−1.06	−1.82	−3.2
A_6	−3.06	−6.08	−1.51	−1.36	−2.31
βN_0(eV)	−2.37[a]	−1.76[b]	−2.48[b]	−1.55[c]	−1.27[d]

[a]Calculated from Eq. (18).
[b]Calculated from Eq. (19).
[c]Interpretation of magneto-optical data (Ref. 22).
[d]From magnetoabsorption (Ref. 94).

*Email address: dietl@ifpan.edu.pl

[1]H. Ohno, H. Munekata, T. Penney, S. von Molnár, and L. L. Chang, Phys. Rev. Lett. **68**, 2664 (1992).
[2]H. Ohno, A. Shen, F. Matsukura, A. Oiwa, A. Endo, S. Katsumoto, and Y. Iye, Appl. Phys. Lett. **69**, 363 (1996).
[3]A. Haury, A. Wasiela, A. Arnoult, J. Cibert, S. Tatarenko, T. Dietl, and Y. Merle d'Aubigné, Phys. Rev. Lett. **79**, 511 (1997).
[4]D. Ferrand, J. Cibert, C. Bourgognon, S. Tatarenko, A. Wasiela, G. Fishman, A. Bonanni, H. Sitter, S. Koleśnik, J. Jaroszyński, A. Barcz, and T. Dietl, J. Cryst. Growth **214/215**, 387 (2000); Physica B **284-288**, 1177 (2000).
[5]See S. Koshihara, A. Oiwa, M. Hirasawa, S. Katsumoto, Y. Iye, C. Urano, H. Takagi, and H. Munekata, Phys. Rev. Lett. **78**, 4617 (1997).
[6]Y. Ohno, D. K. Young, B. Beschoten, F. Matsukura, H. Ohno, and D. D. Awschalom, Nature (London) **402**, 790 (1999).
[7]F. Matsukura, H. Ohno, A. Shen, and Y. Sugawara, Phys. Rev. B **57**, R2037 (1998).

[8] T. Dietl, H. Ohno, F. Matsukura, J. Cibert, and D. Ferrand, Science **287**, 1019 (2000).
[9] H. Ohno, Science **281**, 951 (1998); J. Magn. Magn. Mater. **200**, 110 (1999); J. K. Furdyna, P. Schiffer, Y. Sasaki, S. J. Potashnik, and X. Y. Liu, in *Optical Properties of Semiconductor Nanostructures*, edited by M. L. Sadowski, M. Potemski, and M. Grynberg (Kluwer, Dordrecht, 2000), p. 211.
[10] J. Cibert, P. Kossacki, A. Haury, D. Ferrand, A. Wasiela, Y. Merle d'Aubigné, A. Arnoult, S. Tatarenko, and T. Dietl, in *Proceedings of 24th International Conference on Physics of Semiconductors, Jerusalem, 1998*, edited by D. Gershoni (World Scientific, Singapore, 1999), p. 51.
[11] T. Story, Acta Phys. Pol. A **91**, 173 (1997).
[12] R. Shioda, K. Ando, T. Hayashi, and M. Tanaka, Phys. Rev. B **58**, 1100 (1998).
[13] A. Balzarotti, N. Motta, A. Kisiel, M. Zimnal-Starnawska, M. T. Czyżyk, and M. Podgórny, Phys. Rev. B **31**, 7526 (1985).
[14] A. Oiwa, S. Katsumoto, A. Endo, M. Hirasawa, Y. Iye, H. Ohno, F. Matsukura, A. Shen, and Y. Sugawara, Solid State Commun. **103**, 209 (1997).
[15] A. Van Esch, L. Van Bockstal, J. De Boeck, G. Verbanck, A. S. van Steenbrgen, P. J. Wellmann, B. Grietens, R. Bogaerts, F. Herlach, and G. Borghs, Phys. Rev. B **56**, 13 103 (1997).
[16] H. Shimizu, T. Hayashi, T. Nishinaga, and M. Tanaka, Appl. Phys. Lett. **74**, 398 (1999).
[17] T. Omiya, F. Matsukura, T. Dietl, Y. Ohno, T. Sakon, M. Motokawa, and H. Ohno, Physica E (Amsterdam) **7**, 976 (2000).
[18] W. Walukiewicz, Phys. Rev. B **37**, 4760 (1988).
[19] M. Linnarsson, E. Janzin, B. Monemar, M. Kleverman, and A. Thildekvist, Phys. Rev. B **55**, 6938 (1997).
[20] N. S. Averkiev, A. A. Gutkin, E. B. Osipov, and M. A. Reshchikov, Fiz. Tekh. Poluprovodn. **21**, 1847 (1987) [Sov. Phys. Semicond. **21**, 1119 (1987)].
[21] F. C. Zhang and T. M. Rice, Phys. Rev. B **37**, 3759 (1988).
[22] C. Benoit à la Guillaume, D. Scalbert, and T. Dietl, Phys. Rev. B **46**, 9853 (1992).
[23] A. K. Bhattacharjee and C. Benoit á la Guillaume, Solid State Commun. **113**, 17 (2000).
[24] J. Okabayashi, A. Kimura, O. Rader, T. Mizokawa, A. Fujimori, T. Hayashi, and M. Tanaka, Phys. Rev. B **58**, R4211 (1998).
[25] J. Okabayashi, A. Kimura, T. Mizokawa, A. Fujimori, T. Hayashi, and M. Tanaka, Phys. Rev. B **59**, R2486 (1999).
[26] For a review on diluted magnetic semiconductors, see, e.g., T. Dietl, in *Handbook on Semiconductors*, edited by T.S. Moss (North-Holland, Amsterdam, 1994), Vol. 3b, p. 1251.
[27] W. A. Harrison and G. K. Straub, Phys. Rev. B **36**, 2695 (1987).
[28] H. Akai, Phys. Rev. Lett. **81**, 3002 (1998).
[29] M. A. Paalanen and R. N. Bhatt, Physica B **169**, 153 (1991).
[30] M. Sawicki, T. Dietl, J. Kossut, J. Igalson, T. Wojtowicz, and W. Plesiewicz, Phys. Rev. Lett. **56**, 508 (1986).
[31] P. Głód, T. Dietl, M. Sawicki, and I. Miotkowski, Physica B **194-196**, 995 (1994).
[32] T. Dietl, A. Haury, and Y. Merle d'Aubigné, Phys. Rev. B **55**, R3347 (1997).
[33] T. Jungwirth, W. A. Atkinson, B. H. Lee, and A. H. MacDonald, Phys. Rev. B **59**, 9818 (1999).
[34] D. Belitz and T. R. Kirkpatrick, Rev. Mod. Phys. **57**, 287 (1994), and references therein.
[35] J. Szczytko, K. Świątek, M. Palczewska, A. Twardowski, T. Hayashi, M. Tanaka, and K. Ando, Phys. Rev. B **60**, 8304 (1999).
[36] J. Szczytko, W. Mac, A. Twardowski, F. Matsukura, and H. Ohno, Phys. Rev. B **59**, 12 935 (1999).
[37] B. Beschoten, P. A. Crowell, I. Malajovich, D. D. Awschalom, F. Matskura, A. Shen, and H. Ohno, Phys. Rev. Lett. **83**, 3073 (1999).
[38] G. L. Bir and G.E. Pikus, *Symmetry and Strain-Induced Effects in Semiconductors* (Wiley, New York, 1974).
[39] J. A. Gaj, J. Ginter, and R. R. Gałązka, Phys. Status Solidi B **89**, 655 (1978).
[40] Y. Nishikawa, Y. Satoh, and J. Yoshino (unpublished).
[41] Y. Shapira, S. Foner, P. Becla, D. N. Domingues, M. J. Naughton, and J. S. Brooks, Phys. Rev. B **33**, 356 (1986).
[42] A. Twardowski, P. Świderski, M. von Ortenberg, and R. Pauthenet, Solid State Commun. **50**, 509 (1984).
[43] D. Ferrand, J. Cibert, C. Bourgognon, S. Tatarenko, A. Wasiela, G. Fishman, T. Andrearczyk, S. Koleśnik, J. Jaroszyński, T. Dietl, B. Barbara, and D. Dufeu, cond-mat/0007502 (unpublished); Phys. Rev. B **63**, 085201 (2001); J. Appl. Phys. **87**, 6451 (2000).
[44] P. A. Wolff, R. N. Bhatt, and A. C. Durst, J. Appl. Phys. **79**, 5196 (1996).
[45] R. N. Bhatt and Xin Wan, Int. J. Mod. Phys. C **10**, 1459 (1999).
[46] C. Zener, Phys. Rev. **81**, 440 (1950); **83**, 299 (1951); a similar model for nuclear ferromagnetism was developed by H. Fröhlich and F. R. N. Nabarro, Proc. R. Soc. London, Ser. A **175**, 382 (1940); see also, e.g., P. Leroux-Hugon, in *New Developments in Semiconductors*, edited by P.R. Wallace, R. Harris, and M.J. Zuckermann (Noordhoff, Leyden, 1973), p. 63; M. A. Krivoglaz, Usp. Fiz. Nauk **111** 617 (1973) [Sov. Phys. Usp. **16**, 856 (1974)]; E. A. Pashitskii and S. M. Ryabchenko, Fiz. Tverd. Tela **21**, 545 (1979) [Sov. Phys. Solid State **21**, 322 (1979)].
[47] J. Blinowski, P. Kacman, and J.A. Majewski, in *High Magnetic Fields in Semiconductor Physics II*, edited by G. Landwehr and W. Ossau (World Scientific, Singapore, 1997), p. 861.
[48] T. Dietl, J. Cibert, D. Ferrand, and Y. Merle d'Aubigné, Mater. Sci. Eng., B **63**, 103 (1999), and references therein.
[49] C. Kittel, in *Solid State Physics*, edited by F. Seitz, D. Turnbull, and H. Ehrenreich (Academic, New York, 1968), Vol. 22, p. 1.
[50] U. Larsen, Phys. Lett. **85A**, 471 (1981).
[51] R. Abolfath, T. Jungwirth, J. Brum, and A. H. MacDonald, Phys. Rev. B **63**, 054418 (2001).
[52] W. Szymańska and T. Dietl, J. Phys. Chem. Solids **39**, 1025 (1978).
[53] P. Kossacki, D. Ferrand, A. Arnoult, J. Cibert, S. Tatarenko, A. Wasiela, Y. Merle d'Aubigné, K. Świątek, M. Sawicki, J. Wróbel, W. Bardyszewski, and T. Dietl, Physica E **6**, 709 (2000).
[54] M. E. Fisher, S.-k. Ma, and B. G. Nickel, Phys. Rev. Lett. **29**, 917 (1972).
[55] See J.M. Yeomans, *Statistical Mechanics of Phase Transitions* (Oxford University Press, Oxford, 1993), p. 57.
[56] K. Nishizawa and O. Sakai, Physica B **281-282**, 468 (2000).
[57] M. A. Boselli, A. Ghazali, and I. C. da Cunha Lima, cond-mat/0002254 (unpublished).
[58] J. König, H.-H. Lin, and A. H. MacDonald, Phys. Rev. Lett. **84**, 5628 (2000).
[59] M. Shirai, T. Ogawa, I. Kitagawa, and N. Suzuki, J. Magn. Magn. Mater. **177-181**, 1383 (1998).
[60] R. Kato and H. Katayama-Yoshida (unpublished).

[61] P. T. J. Eggenkamp, H. J. M. Swagten, T. Story, V. I. Litvinov, C. H. W. Swüste, and W. J. M. de Jonge, Phys. Rev. B **51**, 15 250 (1995).
[62] H. Ohno, F. Matsukura, T. Omiya, and N. Akiba, J. Appl. Phys. **85**, 4277 (1999).
[63] H. Ohno, F. Matsukura, A. Shen, Y. Sugawara, A. Oiwa, A. Endo, S. Katsumoto, and Y. Iye, in *Proceedings of the 23rd International Conference on the Physics of Semiconductors, Berlin 1996*, edited by M. Scheffler and R. Zimmermann (World Scientific, Singapore, 1996), p. 405.
[64] A. Hubert and R. Schafer, *Magnetic Domains* (Springer, Berlin, 1998).
[65] D. Bimberg, R. Blachnik, M. Cardona, P. J. Dean, T. Grave, G. Harbeke, K. Huebner, U. Kaufmann, W. Kress, O. Madelung, W. von Muench, U. Roessler, J. Schneider, and M. Schulz, in *Numerical Data and Functional Relationships in Science and Technology*, edited by O. Madelung, M. Schulz, and W. Weiss, Landolt-Börnstein, New Series, Group III, Vol. 17, Pt. a (Springer, Berlin, 1982).
[66] See, *Diluted Magnetic Semiconductors*, edited by J.K. Furdyna and J. Kossut, Vol. 25 of *Semiconductors and Semimetals* (Academic, Boston, 1988).
[67] J. Szczytko, W. Mac, A. Stachow, A. Twardowski, P. Becla, and J. Tworzydło, Solid State Commun. **99**, 927 (1996).
[68] K. Ando, T. Hayashi, M. Tanaka, and A. Twardowski, J. Appl. Phys. **83**, 6548 (1998).
[69] J. Cibert, P. Kossacki, A. Haury, A. Wasiela, Y. Merle d'Aubigné, T. Dietl, A. Arnoult, and S. Tatarenko, in *Proceedings of the International Conference on II-VI Compounds, Grenoble 1997*, edited by R. T. Cox, J. Libert, G. Destefanis, and H. Mariette [J. Cryst. Growth **184/185**, 898 (1998)].
[70] H. C. Casey Jr. and F. F. Stern, J. Appl. Phys. **47**, 631 (1976).
[71] H.C. Casey Jr., D. D. Sell, and K. W. Wecht, J. Appl. Phys. **46**, 250 (1975).
[72] J. A. Gaj, R. Planel, and G. Fishman, Solid State Commun. **29**, 435 (1979).
[73] S. Lankes, M. Meier, T. Reisinger, and W. Gebhard, J. Appl. Phys. **80**, 4049 (1996).
[74] H. W. Hölscher, A. Nöthe, and Ch. Uihlein, Phys. Rev. B **31**, 2379 (1985).
[75] The parameters γ_i of zinc-blende structure ZnS and ZnSe and A_i of wurzite ZnO, CdS, and CdSe were obtained by fitting the corresponding $k \cdot p$ model to the results of band structure computations given by D. Vogel, P. Krüger, and J. Pollmann, Phys. Rev. B **54**, 5495 (1996).
[76] R. Blachnik, J. Chu, R. R. Gałązka, J. Geurts, J. Gutowski, B. Hoenerlage, D. Hofmann, J. Kossut, R. Levy, P. Michler, U. Neukirch, D. Strauch, T. Story, and A. Waag, in *Numerical Data and Functional Relationships in Science and Technology*, edited by U. Rössler, Landolt-Börnstein, New Series, Vol. 41, pt. b (Springer, Berlin, 1999).
[77] H. Venghaus, Phys. Rev. B **19**, 3071 (1979).
[78] T. Mizokawa, J. Okabayashi, T. Nambu, and A. Fujimori (unpublished).
[79] A. Twardowski, M. von Ortenberg, M. Demianiuk, and R. Pauthenet, Solid State Commun. **51**, 849 (1984).
[80] J. Kreissl, W. Ulrici, M. ElMetoui, A. M. Vasson, A. Vasson, and A. Gavaix, Phys. Rev. B **54**, 10 508 (1996).
[81] T. Wojtowicz, T. Dietl, M. Sawicki, W. Plesiewicz, and J. Jaroszyński, Phys. Rev. Lett. **56**, 2419 (1986).
[82] M. Chmielowski, T. Dietl, P. Sobkowicz, and F. Koch, in *Proceedings of the 18th International Conference on the Physics of Semiconductors, Stockholm 1986*, edited by O. Engström (World Scientific, Singapore, 1987), p. 1787.
[83] S. Katsumoto, A. Oiwa, Y. Iye, H. Ohno, F. Matsukura, A. Shen, and Y. Sugawara, Phys. Status Solidi B **205**, 115 (1998).
[84] K. Hirakawa, S. Katsumoto, Y. Hashimoto, and Y. Iye (unpublished).
[85] Y. Nagai, K. Nagasaka, H. Nojiri, M. Motokawa, F. Matsukura, and H. Ohno (unpublished).
[86] T. Kamatani and H. Akai (unpublished).
[87] R. R. Goodman, Phys. Rev. **122**, 397 (1961).
[88] E. O. Kane, J. Phys. Chem. Solids **1**, 249 (1957).
[89] We thank James J. Niggemann for his assistance in the derivation of momentum matrix elements.
[90] I. Broser, R. Broser, H. Finkenrath, R. R. Gałązka, H. E. Gumlich, A. Hoffmann, J. Kossut, E. Mollwo, H. Nelkowski, G. Nimtz, W. von der Osten, M. Rosenzweig, H. J. Schulz, and D. Theis, *Numerical Data and Functional Relationships in Science and Technology*, edited by O. Madelung, M. Schulz, and W. Weiss, Landolt-Börstein, New Series, Group III, Vol. 17, pt. b (Springer, Berlin, 1982).
[91] O. Madelung, W. von der Osten, and U. Rössler, in *Numerical Data and Functional Relationships in Science and Technology*, edited by O. Madelung, Landolt-Börnstein, New Series, Group III, Vol. 22 Pt. (a) (Springer, Berlin, 1987).
[92] K. Kim, W. L. R. Lambrecht, B. Segall, and M. van Schilfgaarde, Phys. Rev. B **56**, 7363 (1997); similar values of the $k \cdot p$ parameters A_i are given by M. Suzuki, T. Uenoyama, and A. Yanase, *ibid.* **53**, 8132 (1995); J. A. Majewski, M. Städele, and P. Vogl, in *III-V Nitrides*, edited by T. Moustakas, B. Monemar, I. Akasaki, and F. Ponce, Mater. Res. Soc. Symp. Proc. Symposia Proceedings **449** (Materials Research Society, Pittsburg, 1997); for a review, see *Properties, Processing and Application of GaN and Related Semiconductors*, edited by J. H. Edgar, S. Strite, I. Akasaki, H. Amano, and C. Wetzel (INSPEC, Stevenager, UK, 1994), pp. 153–207.
[93] Y. C. Yeo, T. C. Chong, and M. F. Li, J. Appl. Phys. **83**, 1429 (1998).
[94] M. Arciszewska and M. Nawrocki, J. Phys. Chem. Solids **47**, 309 (1986).